

Systematic Review on Fabrication, Properties, and Applications of Advanced Materials in Wearable Photoplethysmography Sensors

Mathew, J., Zheng, D., Xu, J. & Liu, H.

Published PDF deposited in Coventry University's Repository

Original citation:

Mathew, J, Zheng, D, Xu, J & Liu, H 2024, 'Systematic Review on Fabrication, Properties, and Applications of Advanced Materials in Wearable Photoplethysmography Sensors', *Advanced Electronic Materials*, vol. (In-Press), 2300765, pp. (In-Press).

<https://dx.doi.org/10.1002/aelm.202300765>

DOI 10.1002/aelm.202300765

ISSN 2199-160X

ESSN 2199-160X

Publisher: Wiley

This is an open access article under the terms of the Creative Commons Attribution License, which permits use, distribution and reproduction in any medium, provided the original work is properly cited.

Systematic Review on Fabrication, Properties, and Applications of Advanced Materials in Wearable Photoplethysmography Sensors

Jinu Mathew, Dingchang Zheng, Jianwei Xu,* and Haipeng Liu*

Photoplethysmography (PPG) technology enables the measurement of multiple physiological and psychological parameters with low-cost wearable sensors and is reshaping modern healthcare. Advanced materials play a vital role in improving reliability and accuracy of PPG sensors. Recently, various advanced materials have been explored to optimize PPG sensor design, while some challenges exist toward large-scale validation and mass production. This paper focuses on advanced materials applied in the photodetectors, light sources, and circuits of PPG sensors. The materials are categorized into four groups: inorganic, organic, nanomaterials, and hybrid materials. The properties and fabrication processes are summarized. Other technical details including the mode of operation, measurement sites, testing, and validation are discussed. The merits and limitations of the state of the art are highlighted to provide some suggestions for the future development of PPG sensors based on advanced materials.

mechanical, electrical, optical, and acoustic ones to monitor different physiological parameters.^[6–8]

Photoplethysmography (PPG) based optical wearable sensing devices are promising wearable sensors with unique advantages. One of the main advantages of PPG devices is the extraction of multiple physiological parameters in relation to the cardiovascular system (e.g., heart rate, BP, oxygen saturation, and arterial stiffness),^[9] respiratory system (respiration rate),^[10] and neurological system (e.g., mental stress and stage of sleep).^[11–14] With the development of sensor design and signal processing algorithms, PPG shows great potential in daily healthcare monitoring and clinical diagnosis of multiple (cardiovascular,

1. Introduction

Wearable sensing technologies have boomed over the past decade. Nowadays these devices become a part of our bodies in the form of smartwatches, smartphones, and other smart garments. Aside from having an aesthetic appearance, wearable sensing devices are primarily used for regular monitoring of human health signs like heart rate, blood pressure (BP), body temperature, respiratory rate, mental stress, and oxygen saturation in blood.^[1–5] These devices use various signals including


respiratory, neurological, diabetic, and skin) diseases and psychological disorders, with emerging clinical applications in patient screening (e.g., COVID-19 and atrial fibrillation) and treatment efficiency evaluation (e.g., dialysis and surgery).^[9] PPG technology is playing an increasingly important role in modern wearable healthcare. Especially, the recent development of wearable electronics is leading revolutionary changes of PPG technology toward higher signal quality and clinical applicability based on biocompatible, high-performance, and ultra-lightweight PPG devices.^[15]

A typical PPG device mainly consists of a light source, a substrate on which the sensing layer (photodetector) is patterned, and a printed circuit board. As shown in **Figure 1a**, PPG sensors measure the intensity of light transmitted or reflected with respect to the changes in the volume of blood flowing through the blood vessels. Light sources with different wavelengths are selected based on the mode of operation (transmission or reflection) and the depth of measurement (**Figure 1b**).^[12] The reflected or the transmitted light that falls on the photodetector is converted into electric energy and amplified using electrical circuits to generate the waveform (**Figure 1c**).^[16]

Materials used in the fabrication of PPG devices play a vital role in making the device more reliable, accurate, and user-friendly. The substrate of the PPG sensor should be biocompatible, flexible, and stretchable. The materials for sensing layer (photodetector) should be sensitive and robust against noises. The electronic circuit of a preferred PPG device is highly integrated, flexible, with reliable performance in different strain conditions.^[17] Apart

J. Mathew, D. Zheng, H. Liu
Research Centre for Intelligent Healthcare
Coventry University
Coventry CV1 5RW, UK
E-mail: haipeng.liu@coventry.ac.uk

J. Xu
Institute of Materials Research and Engineering
A*STAR (Agency for Science, Technology and Research)
2 Fusionopolis Way, Innovis #08-03, Singapore 138634, Singapore
E-mail: xu_jianwei@isce2.a-star.edu.sg

 The ORCID identification number(s) for the author(s) of this article can be found under <https://doi.org/10.1002/aelm.202300765>

© 2024 The Authors. Advanced Electronic Materials published by Wiley-VCH GmbH. This is an open access article under the terms of the [Creative Commons Attribution](https://creativecommons.org/licenses/by/4.0/) License, which permits use, distribution and reproduction in any medium, provided the original work is properly cited.

DOI: 10.1002/aelm.202300765

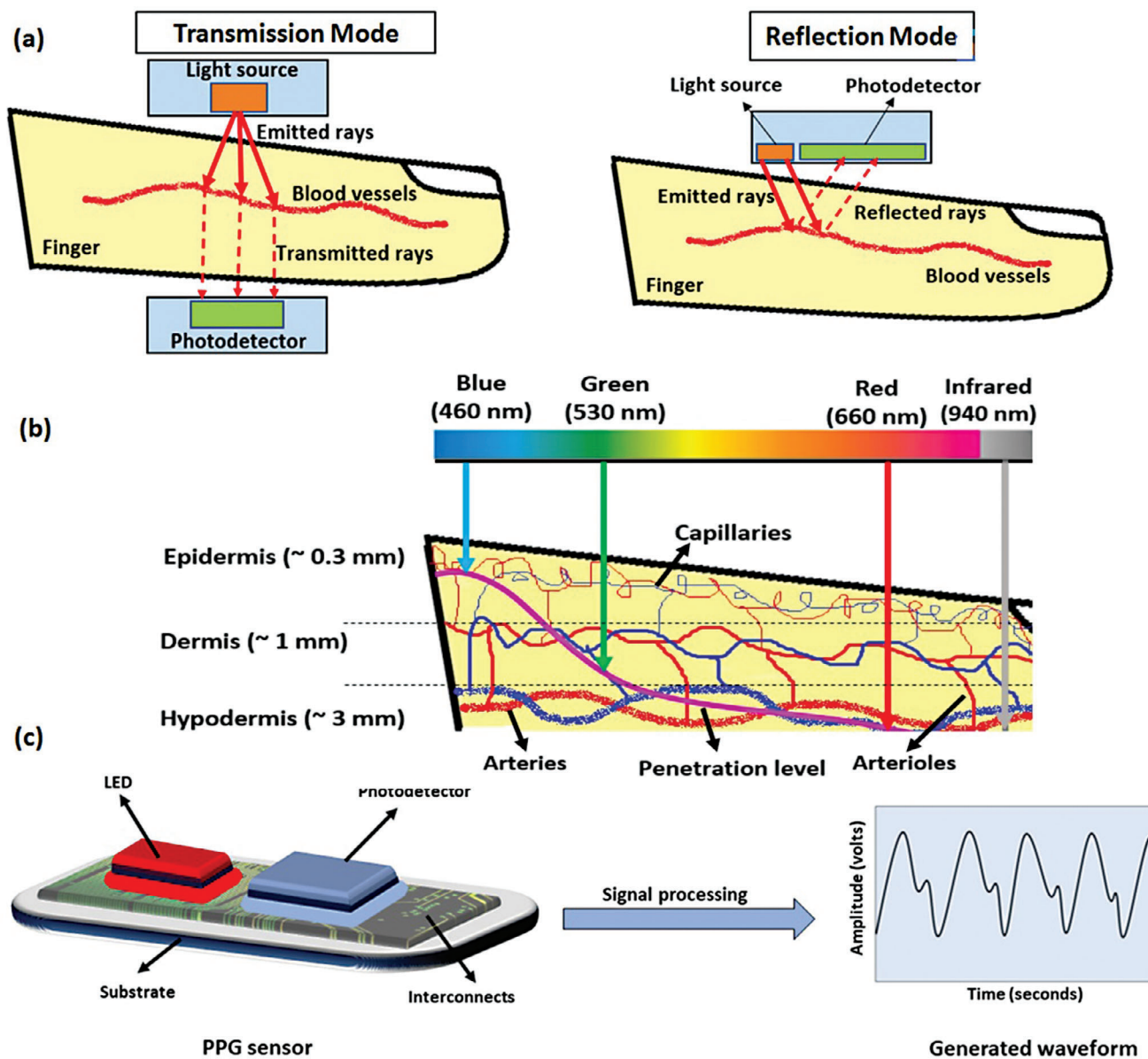


Figure 1. a) Mode of operation of PPG sensors. b) Different light sources used in PPG. c) PPG hardware.

from these properties, the whole device should be possibly miniaturized and aesthetic.^[18] Therefore, materials used in the fabrications of PPG devices should be selected carefully to achieve the best overall performance.

A major limitation of current PPG devices is the sensitivity to noises including motions and surrounding light, which distorts the PPG signals and leads to erroneous readings.^[19] To address this issue, many different techniques have been developed, such as advanced de-noising algorithms,^[20–22] multi-wavelength sensing (green, red, visible, infra-red light),^[23,24] and using materials with better biomechanical and optic properties.^[17,25–27] Among them, better materials may provide the fundamental solution and bring other preferred properties including waterproofing, biocompatibility and comfortability.

Some researchers have reviewed the materials used in PPG sensors, focusing on organic materials used in certain applications such as oxygen saturation.^[28,29] Whereas, there is a scarcity of comprehensive review on advanced materials in different components of PPG sensors with different applications scenarios. In comparison, some comprehensive review studies are available on PPG signal processing and multi-wavelength sensing.^[12,16,22,23,30] To address this gap, we reviewed different materials used in current PPG sensors and classified them into different groups: organic materials, inorganic materials, nanomaterials, and hybrid materials. We first summarized the materials, their properties, and fabrication procedures. We discussed the lab tests, relevant physiological parameters and applications scenarios of different materials for PPG devices, and extracted the advantages,

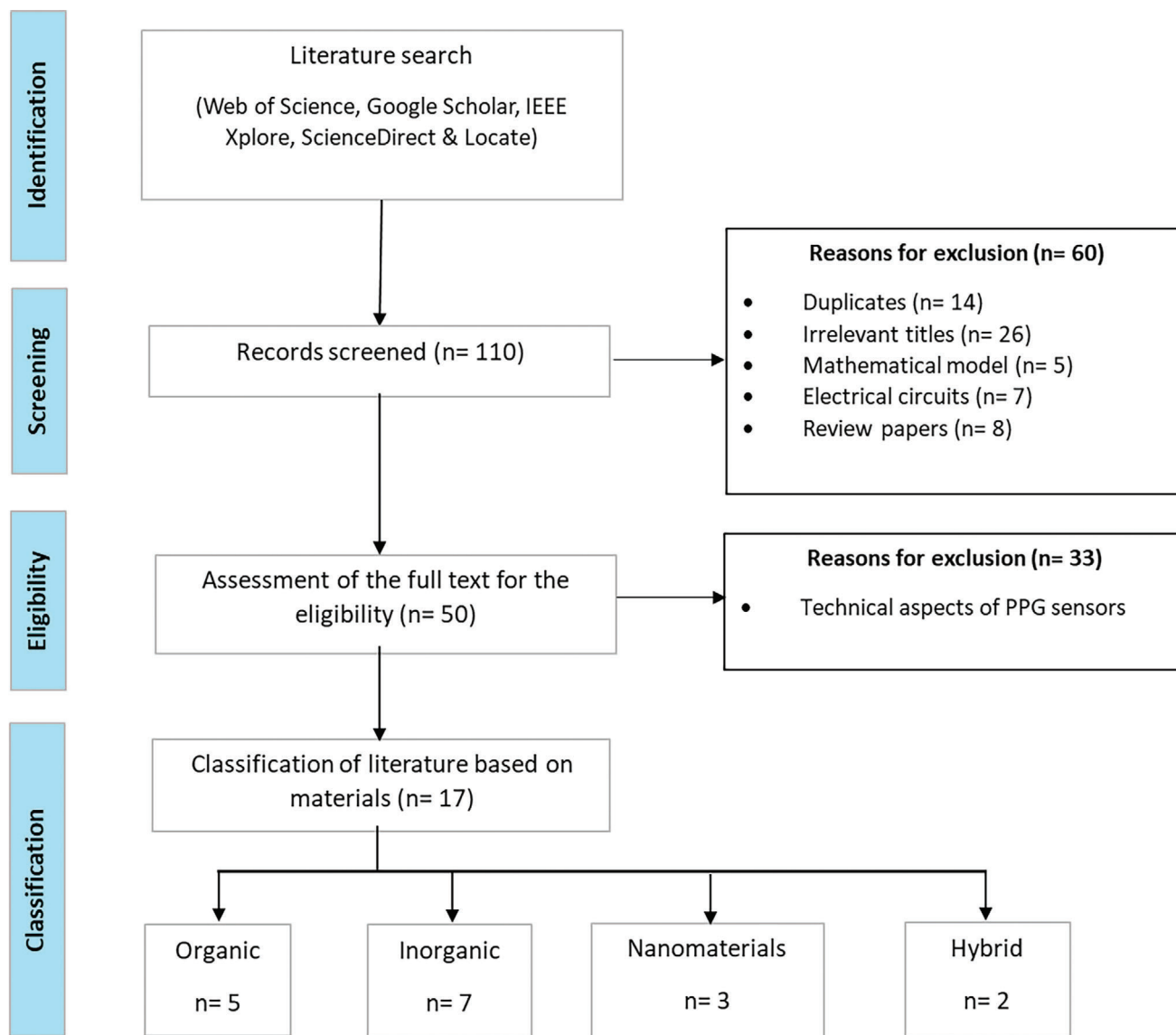


Figure 2. Literature search and classification strategy.

limitations, and future directions. This systematic review serves as a valuable guide for developing next-generation PPG sensors with enhanced performance, leveraging novel materials to achieve more desired functions.

2. Literature Search Strategy

The literature search strategies used in this paper are presented in **Figure 2**. Databases including Web of Science, IEEE Xplore, ScienceDirect, locate (University library website), and Google Scholar were used for the literature search. The retrieval time was from the establishment of the database to 1st July 2023. The language was restricted to English. Keywords were combined using Boolean operators. Synonyms were combined using “OR” operator in different groups. Then, the three groups were combined using “AND” operator.

Group 1: “Photoplethysmography” or “PPG” or “Photoplethysmograph”.

Group 2: “Organic” or “Inorganic” or “Nanomaterials” or “Hybrid”

Group 3: “Wearable” or “Flexible” or “Stretchable”

A total of 110 articles were found in a systematic search. In the collected papers, 60 literatures were screened out since these have irrelevant titles, duplicates, review papers, focused on mathematical models, or electrical circuits of PPG. After a brief review of the remaining selected 50 works, they were categorized into two groups based on materials used and technical aspects of PPG devices. The publications on the materials used in the PPG sensors are further categorized based on organic, inorganic, nanomaterials and hybrids. A detailed analysis and discussions based on these categories were done in the following sections of this review paper.

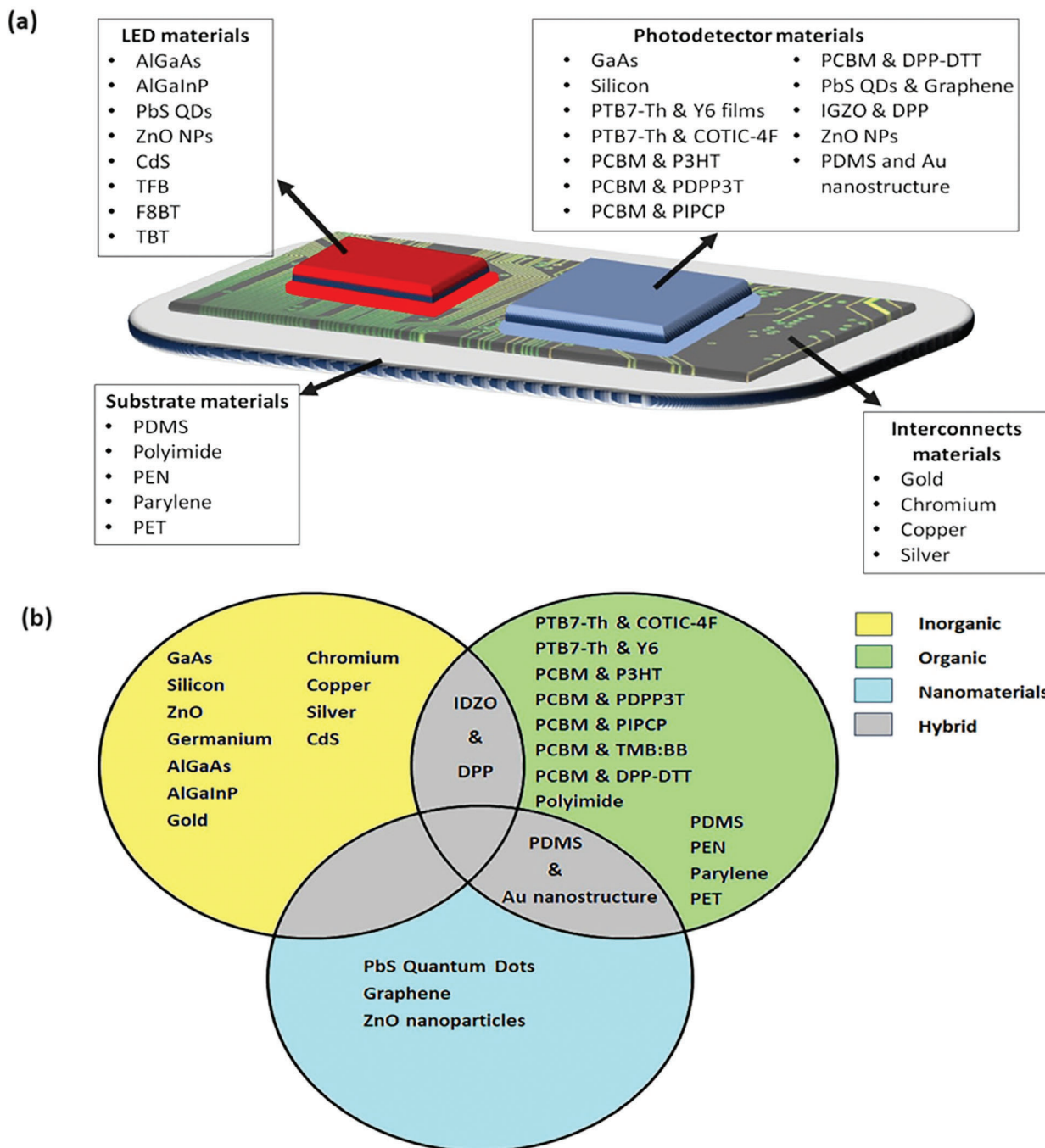


Figure 3. a) Materials used in the fabrication of different parts of a PPG device. b) Classification of materials used in PPG devices.

3. Materials in PPG Sensors: Properties and Fabrications

As aforementioned, the selection of materials of PPG sensor fabrication depends on the biomechanical and optical properties. **Figure 3a,b** illustrate various materials used in the fabrication of main parts of PPG devices studied in this paper.

The majority of the off-the-shelf PPG devices are made of inorganic materials, e.g., silicon (Si), gallium arsenide (GaAs), zinc

oxide (ZnO), and germanium where Si is the commonest since it is widely available, low-cost, non-toxic, with high electron mobility and an indirect band gap. Materials having indirect band gaps allow the PPG sensor to tailor its sensitivity to a certain wavelength range, primarily red and infrared, and enhance charge carrier recombination.^[31] This wavelength range corresponds to hemoglobin's absorption characteristics, making it beneficial for reliable and accurate PPG signal acquisition. Although widely used, most inorganic materials in the PPG technology are fragile,

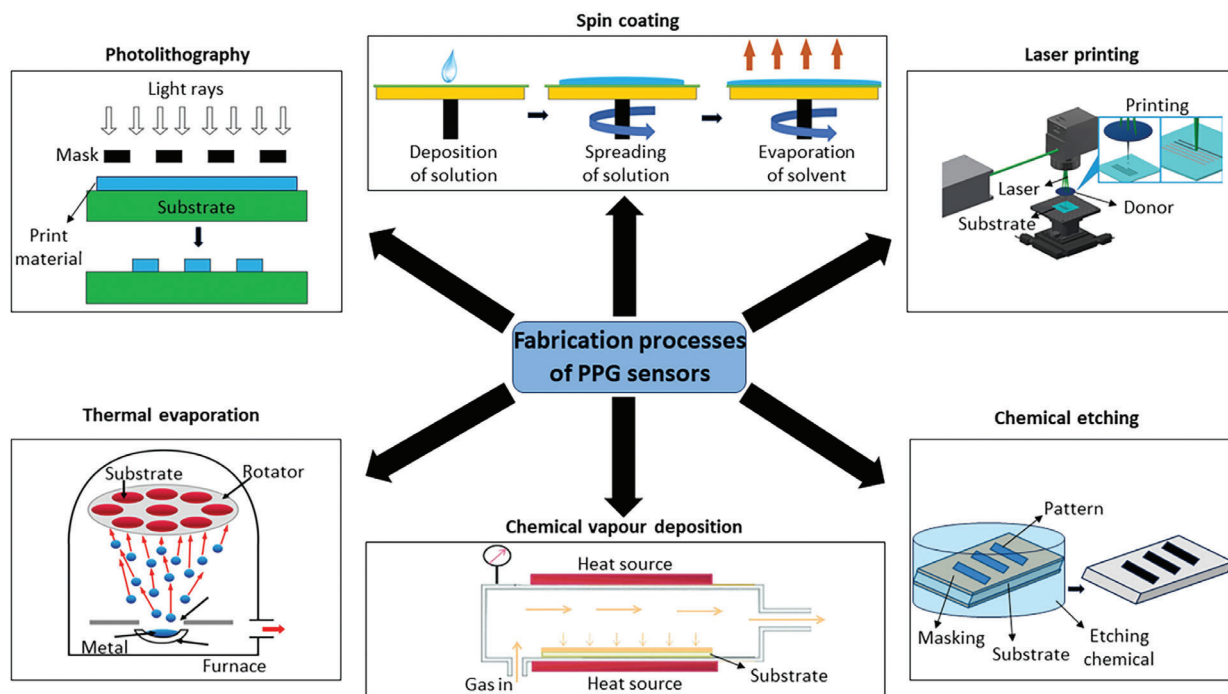


Figure 4. Different processes involved in the fabrication of PPG sensors (adapted from;^[37–41] Thermal evaporation- Reproduced under terms of the CC-BY license.^[37] Copyright 2019, The Authors, published by MDPI; Laser printing- Reproduced under terms of the CC-BY license.^[38] The Authors, published by MDPI; Spin coating- Reproduced under terms of the CC-BY license.^[39] The Authors, published by MDPI; Chemical vapour deposition- Reproduced under terms of the CC-BY license.^[40] The Authors, published by MDPI; Photolithography- Adapted under the terms of CC-BY license.^[41] The Authors, published by Hindawi).

sensitive to noise artifacts, not conformable to the skin, and often require a rigid substrate and layers to produce good responsivity to blood volume changes.^[26,32,33]

To overcome the limitations of inorganic materials, some researchers explored organic semiconducting materials and polymers, e.g., Poly ([2,6'-4,8di (5-ethyl hexyl thienyl) benzo[1,2-b;3,3-b] dithiophene]-thorium (PTB7), PCBM, Poly(3-hexylthiophene-2,5-diyl) (P3HT), Poly[[2,5-bis(2-hexyldecyl)-2,3,5,6-tetrahydro-3,6-dioxopyrrolo [3,4-c] pyrrole-1,4-diyl]-alt-[2,2':5',2"-terthiophene]-5,5"-diyl] (PDPP3T), poly indacenodithio- phene-pyridyl [2,1,3] thiadiazole- cyclopenta di-thiophene (PIPCP), 3,3',5,5'-tetramethylbenzidine: Benzyl benzoate (TMB:BB), and Poly (N-alkyl diketopyrrolo-pyrrole dithienylthieno[3, 2-b]thiophene) (DPP-DTT) in various PPG devices. PCBM and PTB7 are polymers with a wide range of light absorption and good charge mobility, therefore widely used. In comparison with inorganic materials, organic materials used in PPG devices are more biocompatible, economical, and require a thin substrate, and conformable with skin.^[34] However, most organic material-based PPG sensors have suffered from instability and limited charge mobility.^[29] To compensate for organic materials' low charge mobility, appropriate molecules are doped or sandwiched with high charge mobility materials. However, these solutions sacrifice the device's flexibility, thickness, and complexity in order to achieve improved charge mobility.^[35] Some nanomaterials including lead sulphide (Pbs) quantum dots (QDs), graphene, and ZnO nanoparticles (NPs) have been used to improve the optic and electronic properties of PPG photodetectors, such as increasing light absorption at specific

wavelengths, reducing noise in PPG signals, miniaturizing the sensor, and improving response time to changes in physiological parameters.^[36] The degree of improvement in these attributes is measure by the nanomaterials employed, the processing involved, the design of the device, and other manufacturing parameters. To combine the excellent properties of different materials, some researchers developed hybrid materials and applied them in PPG sensors.

The substrate, electrodes, active layer, and encapsulation layer are the main parts of a photodetector. Similarly, LEDs consist of a substrate, a light-emitting active layer, and electrodes. Circuits and interconnects are employed to connect different parts of the sensor, process the signals, and give the output. Apart from the materials used, fabrication and assembling processes adopted in various components of a PPG device play a vital role in the smooth functioning of the sensor. Photolithography, spin coating, laser printing, chemical etching, thermal evaporation, and chemical vapor deposition are a few manufacturing strategies used in different PPG sensors. The illustrations of these processes are demonstrated in **Figure 4**.

3.1. Materials used in the Fabrication of Photodetector of PPG Devices

The ability of photodetector to sense reflected or transmitted light from the measurement sites of physiological parameters is highly related to the overall performance of a PPG device. Therefore, many researchers have studied different materials that can be

used in the photodetectors. **Table 1** summarizes various materials and their properties used in the fabrication of photodetectors of various PPG devices.

3.1.1. Inorganic Materials

GaAs: GaAs is an inorganic semiconductor material with a direct band gap of 1.4 eV, a high electron mobility of $8500 \text{ cm}^2 \text{ V}^{-1} \text{ s}^{-1}$, a high breakdown voltage of $4 \times 10^5 \text{ V cm}^{-1}$, good thermal insulation and moisture resistance.^[42] GaAs is used in many electronic circuits and devices as a substitute to Si.

Kim et al.^[43] developed a PPG device with a GaAs-based photodetector to monitor the human heart rate from various body locations including finger, fingertip, and forearm. They utilized the wet chemical etching process for the fabrication of GaAs. The photodetectors were fabricated in arrays (**Figure 5**). An N-doped GaAs contact layer of the photodetector was metal-deposited followed by wet chemical etching process. Then, with the help of photolithography and mesa-etching, an active region of $760 \mu\text{m} \times 720 \mu\text{m}$ was developed. An equivalent sized p-doped GaAs bottom contact layer was developed by photolithography, metal deposition and lift-off process. With spin coating, the fabricated contact layers of the GaAs were reinforced by an epoxy layer in rectangular patterns with holes. Four such reinforced GaAs photodetectors were fetched by contacting the GaAs substrate with polydimethylsiloxane (PDMS) stamp and the fetched arrays were printed on polyimide with the help of an adhesive layer of SU-8. To improve the sensitivity by increasing the photocurrent, the four printed photodetectors were interconnected in parallel series.

The top and bottom layers of the fabricated sensor were covered with layers of tacky silicone elastomer (Ecoflex) to enhance skin conformability. The light source used was a red LED of wavelength 620 nm. It was integrated to the sensor with the help of sputtered electrical interconnects. The entire system was then encapsulated in PDMS layers to make the device biocompatible.

The flexibility of the fabricated device was evaluated by bending test and the corresponding J-V characteristics of the sensor was plotted before, during, and after bending. The curves were almost identical in all the cases. Electrical characteristics like short circuit current and current density- voltage were studied by LED irradiation and a source measure unit. The fabricated sensor was validated in different physiological conditions (relaxing and after running).

Silicon: Si is the most abundant element in the earth's crust after oxygen. It is widely available and economically affordable. Si is a non-toxic semiconductor material having an indirect band gap of 1.12 eV, high electron mobility ($1400 \text{ cm}^2 \text{ V}^{-1} \text{ s}^{-1}$), high breakdown voltage ($3 \times 10^5 \text{ V cm}^{-1}$), and good thermal conductivity of $1.5 \text{ W cm}^{-1} \text{ K}^{-1}$.^[58] These properties of Si make it the commonest semiconductor in the photodetectors of PPG devices.

Kim et al.^[44] and Kim et al.^[46] conducted separate studies to develop battery-free wireless Si based PPG sensors. In both studies, commercially bought Si-based PPG sensors were coupled with Cu coils to achieve near field battery-free wireless communication with smartphones. Kim et al.^[44] coupled the PPG sensor with temperature sensor and conducted finite element anal-

ysis on the device layout to achieve best system-level elastic responses for accommodating large strain deformations. The fabricated device was then used to measure heart rate, oxygen saturation level in blood, color spectroscopic evaluation of skin and ultraviolet dosimetry. On the other hand, Kim et al.^[46] focused on the miniaturization of the Si-based PPG device to measure blood oxygenation level, heart rate and heart rate variability from fingernails and toenails aiming to ensure extended operational duration with minimal motion artifacts and reduced irritation for the end user. This was achieved by using a multilayer layout with a bilayer loop antenna and an opaque encapsulation layer on the outer surface of the photodetector. These two modifications improved the maximum energy efficiency of the device and provided excellent protection against ambient light and other noises.

Li et al.^[45] designed a new Si-based PPG device to reduce the brittleness of the Si semiconductor and to boost the adaptability of the photodetector to the changes of light intensity induced by skin deformation. To achieve this, the authors used nanodiamond thinning process, specific strain-isolation design, and hybrid transfer printing in sensor fabrication. Specific strain isolation was attained by suspending the whole device in a viscous fluid chamber consisting of cured liquid PDMS and polyurethane film (**Figure 6**). As a result, the distance between the LEDs and the photodetector remained constant even if the device is subjected to stretching and bending due to body movements. To obtain an ultrathin photodetector, they used the nanodiamond grinding technique rather than the traditional chemical etching process and thereby developed the photodetector with a thickness of $17.78 \mu\text{m}$. Fallica et al.^[27] developed a miniaturized Si PPG sensor coupled with electrocardiograph signals to measure the heart rate variability of humans. Each probe of the sensor was inserted in a cuff that can exert adjustable pressure. Also, the system used a band-pass digital filter to remove the unwanted signals from the PPG. They focused more on microelectronic circuits to miniaturize the device and tested it on 12 human subjects with different ages. Both devices^[27,45] used red and infrared LEDs, while the Si photodetector operated on the reflection mode.

3.1.2. Organic Materials

PPG sensors made of different organic materials have recently gained the attention among many researchers due to numerous advantages such as low cost, ease of processing for sensor fabrication, and high flexibility.^[17] PTB7-Th, COTIC-4F, PCBM, P3HT, PDPP3T, PIPCP, TMB:BB, and DPP-DTT are a few organic materials/polymers that are used in different PPG devices.

PTB7-Th in Combination with COTIC-4F and Y6: PTB7-Th is a polymer with a wide range of absorption from green to near infrared (NIR) bands.^[59] COTIC-4F is an n-type semiconductor polymer having a narrow bandgap of $\approx 1.1 \text{ eV}$ and absorption between 700 and 1100 nm.^[60] Y6 is a highly conjugated electron-accepting organic semiconductor composed of a fused thienothiopyrrolo-thienothiaindole core base and 2-(5,6-difluoro-3-oxo-2,3-dihydro-1H-inden-1-ylidene) malononitrile end units.^[61] These organic materials are used in many organic solar cells and photodetectors as an active material layer.

Table 1. Materials and their properties used in the fabrication of photodetectors of various PPG sensors.

Materials	Properties	PPG sensor type & light source	Reference	
Inorganic	GaAs	<ul style="list-style-type: none"> Semiconductor Direct band gap (1.4 eV) High electron mobility (8500 cm² V⁻¹ s⁻¹) High breakdown voltages (4*10⁵ V cm⁻¹) Good thermal and moisture resistance 	<ul style="list-style-type: none"> Reflection mode Light source: Red LED 	[43]
	Silicon	<ul style="list-style-type: none"> Semiconductor Non-toxic 2nd most abundant element in earth's crust Indirect band gap (1.12 eV) High electron mobility (1400 cm² V⁻¹ s⁻¹) High breakdown voltage (3*10⁵ V cm⁻¹) Good thermal conductivity (1.5 W cm⁻¹ K⁻¹) 	<ul style="list-style-type: none"> Reflection mode Light source: Infrared 	[44]
		<ul style="list-style-type: none"> Reflection mode Light source: Red LED Infrared 	[45]	
Organic	PTB7-Th & COTIC-4F	<ul style="list-style-type: none"> Wide range of absorption (Green to near-infrared (NIR)) p-type semiconductor n-type semiconductor Narrow bandgap (1.1 eV) 	<ul style="list-style-type: none"> Reflection mode Light source: Red LED Infrared 	[46]
	PTB7-Th & Y6 films	<ul style="list-style-type: none"> Wide range of absorption (Green to NIR) p-type semiconductor n-type semiconductor High absorption coefficient 	<ul style="list-style-type: none"> Reflection mode Light source: Red LED Infrared 	[27]
	PCBM & P3HT	<ul style="list-style-type: none"> n-type fullerene semiconductor Electron mobility of 10⁻³ cm² V⁻¹ s⁻¹ Regioregular semiconductor Energy band gap of 1.9 eV Electron mobility of 0.12 cm² V⁻¹ s⁻¹ 	<ul style="list-style-type: none"> Transmission mode Light source: Red LED Infrared 	[26]
	PCBM & PDPP3T	<ul style="list-style-type: none"> Wide range of absorption (Green to NIR) p-type semiconductor n-type semiconductor High absorption coefficient 	<ul style="list-style-type: none"> Transmission mode Light source: Infrared LED 	[47]
	PCBM & PIPCP	<ul style="list-style-type: none"> n-type fullerene semiconductor Electron mobility of 10⁻³ cm² V⁻¹ s⁻¹ Band gap of 1.34 eV Hole mobility of ≈0.04 cm² V⁻¹ s⁻¹ 	<ul style="list-style-type: none"> Reflection mode Light source: Blue LED Green LED Red LED 	[48]
	PCBM & TMB:BB	<ul style="list-style-type: none"> n-type fullerene semiconductor Electron mobility of 10⁻³ cm² V⁻¹ s⁻¹ Colorless visualization reagent Colorless and insoluble in water Commonly used for medical purposes 	<ul style="list-style-type: none"> Reflection mode Light source: Red LED NIR LED 	[49]
	PCBM & DPP-DTT	<ul style="list-style-type: none"> n-type fullerene semiconductor Electron mobility of 10⁻³ cm² V⁻¹ s⁻¹ p-type semiconductor Good air stability Good hole mobility (0.5 to 3 cm² V⁻¹ s⁻¹) 	<ul style="list-style-type: none"> Reflection mode Light source: NIR LED 	[50]
	PCBM & PIPCP	<ul style="list-style-type: none"> n-type fullerene semiconductor Electron mobility of 10⁻³ cm² V⁻¹ s⁻¹ Regioregular semiconductor Narrow band gap (1.5 eV) Good solution processibility 	<ul style="list-style-type: none"> Mode: Not mentioned Light source: Infrared LED 	[51]
Nanomaterials	PbS QDs & Graphene	<ul style="list-style-type: none"> Inorganic semiconductor Band gap of 1.2 eV Chemical inertness and high surface activities Honeycomb structure Good electrical conductivity (1732 S m⁻¹) Excellent mechanical strength (≈125 GPa) 	<ul style="list-style-type: none"> Reflection mode Light source: Red LED 	[52]
		<ul style="list-style-type: none"> Transmission mode Light source: Blue LED Green LED Red LED 	[53]	

(Continued)

Table 1. (Continued)

Materials	Properties	PPG sensor type & light source	Reference
		<ul style="list-style-type: none"> • Transmission mode • Reflection mode • Light source Green LED Ambient light Red light NIR 	[54]
	ZnO NPs	<ul style="list-style-type: none"> • Wurtzite n-type semiconductor • High exciton binding energy (60 meV) • Wide band gap (3.37 eV) 	[55]
Hybrid materials	IGZO & DPP	<ul style="list-style-type: none"> • Amorphous inorganic n-type semiconductor • Band gap of 3.05 eV • Electron mobility of $10 \text{ cm}^2 \text{ V}^{-1} \text{ s}^{-1}$ • Organic p-type semiconductor • Widely used as a dye polymer 	[56]
	Au nanostructure & PDMS	<ul style="list-style-type: none"> • Size tunable luminescence • Plasmon color property • Organic Si-based polymer • Non-toxic and non-flammable • Hydrophobic 	[57]

Simoes et al.^[26] fabricated a PPG sensor using a bulk heterojunction blend of PTB7-Th and COTIC-4F organic functional material on polyethylene naphthalate (PEN) substrate with a bottom indium tin oxide (ITO) anode and a top layer of aluminum cathode (Figure 7a). Interfacial layers of Poly (3,4-ethylene dioxythiophene) polystyrene sulfonate (PEDOT: PSS) and N, N'-Bis (N, N-dimethylpropan-1-amine oxide) perylene-3,4,9,10-tetracarboxylic di-imide (PDINO) were placed on the bottom and top of the photodetector respectively to suppress the undesired carrier injection. Similarly, Eun et al.^[47] developed an organic PPG sensor by using Y6 instead of COTIC-4F to make the bulk heterojunction active layer on a parylene substrate (Figure 7f). ITO and silver were used as the bottom anode and top cathode layers, respectively. As the interfacial layers, Eun et al.^[47] used ZnO and molybdenum oxide. Both researchers used different technique like spin coating, thermal annealing, and ther-

mal evaporation for the fabrication of different layers of the photodetectors.

Regarding the derived PPG sensors, Simoes et al.^[26] used red and NIR LEDs, whereas Eun et al.^[47] used only one infrared light source at 851 nm. Simoes et al.^[26] measured oxygen saturation in blood and heart rate from one human subject at rest for 180 s and the readings were validated with a commercially available PPG device. Eun et al.^[47] measured the heart rate of a healthy human subject at normal conditions and compared the obtained values with standard values. Both fabricated PPG devices worked in the transmission mode.

PC_xBM in Combination with P3HT, PDPP3T, PIPCP, TMB:BB, and DPP-DTT: PC_xBM is a fullerene-based electron-accepting material widely used in organic solar cells. It has an electron mobility of $10^{-3} \text{ cm}^2 \text{ V}^{-1} \text{ s}^{-1}$.^[62] C_x indicates the type of carbon fullerene and the most commonly used are C₆₀, C₆₁, and C₇₁. When PC_xBM is used as an electron acceptor in optoelectronic

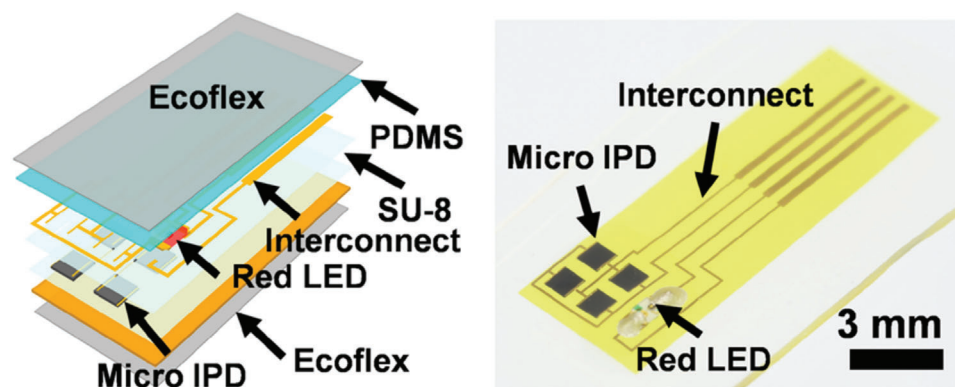


Figure 5. Schematic illustration of attachable pulse sensor designed by Kim et al.^[43] (IPD: Inorganic photodetector; Reprinted with permission.^[43] Copyright 2017, American Chemical Society).

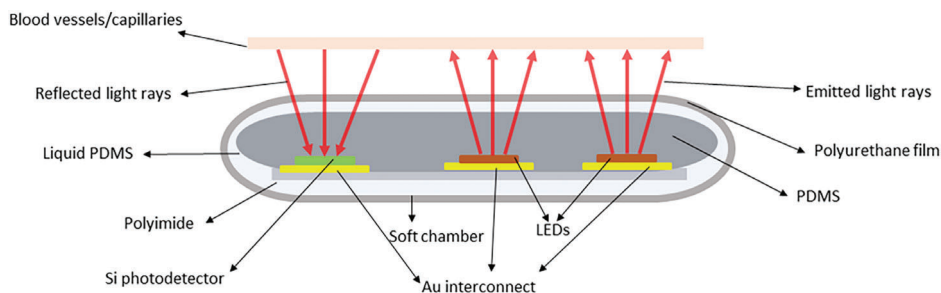


Figure 6. The illustration of an all-in-one suspension structure.^[45]

devices, it allows efficient and rapid charge transfer and exciton dissociation.

P3HT is a regioregular organic electron-donating polymer with a low energy band gap (≈ 1.9 eV) and electron mobility of $0.12 \text{ cm}^2 \text{ V}^{-1} \text{ s}^{-1}$.^[63] In addition to good hole mobility and good solubility, P3HT has good air stability in comparison with other photosensitive polymers, and this makes P3HT popular in optoelectronic devices.^[64] PDPP3T is an electron-rich polymer with a good hole mobility of $\approx 0.04 \text{ cm}^2 \text{ V}^{-1} \text{ s}^{-1}$ and a band gap of 1.34 eV.^[65] PIPCP is a regioregular polymer having a narrow band gap of 1.5 eV.^[66] It is used with other electron-accepting polymers to fabricate the photosensitive layers of optoelectronic devices. TMB is a colorless polymer commonly used as a visualization reagent in many enzyme-catalytic reactions. When oxidized, it turns to blue color, and yellow in the presence of acids.^[67] Benzyl benzoate (BB) is an organic compound commonly used in skin care, medications, and insect repellents. It can alter and impart desired properties of other compounds and polymers.^[68] DPP-DTT is a p-type semiconducting polymer having high hole mobility (0.5 to $3 \text{ cm}^2 \text{ V}^{-1} \text{ s}^{-1}$) and good air stability.^[69] It is widely used as a donor material in bulk heterojunction with other polymers in solar cells, photodetectors, and other sensing applications. The chemical structures of PCBM, P3HT, PDPP3T, PIPCP, TMB, and DPP-DTT are shown in **Figure 8**. Yokota et al.^[48], Simone et al.,^[49] Park et al.,^[50] Khan et al.,^[51] and Xu et al.^[52] fabricated different PPG devices based on PCBM in combination with different polymers and compounds that are mentioned herewith.

Yokota et al.^[48] developed an ultra-flexible organic PPG sensor using multi-color polymer LEDs (PLED) and a photodetector with a blend of PCBM and P3HT. The organic photodetector was made on a parylene substrate and used ITO as the cathode electrode (**Figure 7b**). Then, interfacial layers of thin ethoxylated polyethyleneimine were deposited by spin coating. On top of it, the active layer of P3HT: PCBM was spin-coated, followed by thermal evaporation of MoO_x and Au as the anode electrode. The photodetector was passivated by a thick layer of parylene. Simone et al.^[49] developed a PPG array using a blend of PDPP3T and PC_{61}BM organic photodiodes (**Figure 7c**). They photolithographically patterned chromium molybdenum alloy film on a glass substrate to form the bottom anode. The active layer of PDPP3T: PC_{61}BM was deposited by spin coating on the interfacial layer of amorphous indium zinc oxide. The top electrode made of MoO_x and Ag was deposited by thermal evaporation on the photodetector.

The devices developed by Yokota et al.^[48] and Simone et al.^[49] operated in a reflection mode to measure blood oxygen satura-

tion levels from fingers. In both cases, the readings were taken from one human subject, and these were validated using commercial pulse oximeters. Yokota et al.^[48] conducted cyclic testing on the device to assess the mechanical flexibility and stability. On the other hand, Simone et al.^[49] used green, red, and NIR LEDs up to 950 nm as the light source. Apart from this, Simone et al.^[49] designed the photodetector in small arrays and used the pixel averaging technique to extract high-quality PPG waveforms to yield information on the stiffness of the arteries and the quality of blood circulation.

Park et al.^[50] developed a NIR sensitive PPG device incorporated with a photodetector active layer composed of PIPCP and PC_{61}BM blend (**Figure 7d**). The photodetector was made on a glass substrate spin-coated with a fluorinated polymer layer and a thin layer of chemical vapor deposited parylene film. Planarization was obtained by spin coating a 500 nm thick epoxy layer. ITO and a layer of MoO_x and Ag were used as the bottom and the top electrodes respectively. On the top of ITO, a thin layer of ZnO layer was spin-coated, and the active layer of PIPCP: PC_{61}BM was deposited in a glove box. The chemical vapor-deposited parylene layer was used as the passivation layer of the photodetector. In another example, Khan et al.^[51] developed a PPG device having photodetectors made from PC_{71}BM and TMB:BB polymers (**Figure 8e**). The organic photodetectors were fabricated on a PEN substrate where PEDOT: PSS was blade coated as the anode. On the top of the anode, the active layer of PC_{71}BM and TMB: BB was deposited by blade coating. Then, silver traces were screen printed as in the fabricated LEDs. Finally, a top layer of the aluminum cathode was deposited by thermal evaporation to complete the photodetector stacks. The fabricated LEDs and photodetectors were assembled to form a reflective oximeter array in four rows. The reflective oximeter array consisted of eight photodetectors and eight LEDs (four red LEDs and four NIR LEDs).

Park et al.^[50] measured the circuit current, circuit voltage, and pulse waves from the fingertip of a human subject before and after severe mechanical deformation on the PPG sensor. Also, they conducted a bending test on the fabricated device for 1000 cycles. From all these experiments, they showed that their PPG device was flexible, skin conformal, and mechanically stable. Khan et al.^[51] calculated the blood oxygen saturation with the fabricated PPG device from the forehead and fingers of a human subject. The obtained readings were validated by comparing them with the outputs from a transmission-mode commercial pulse oximeter. Because of the peculiar design of the reflective oximeter array, they were also efficient to plot a 2D blood oxygen saturation map under pressure cuff-induced ischemia.

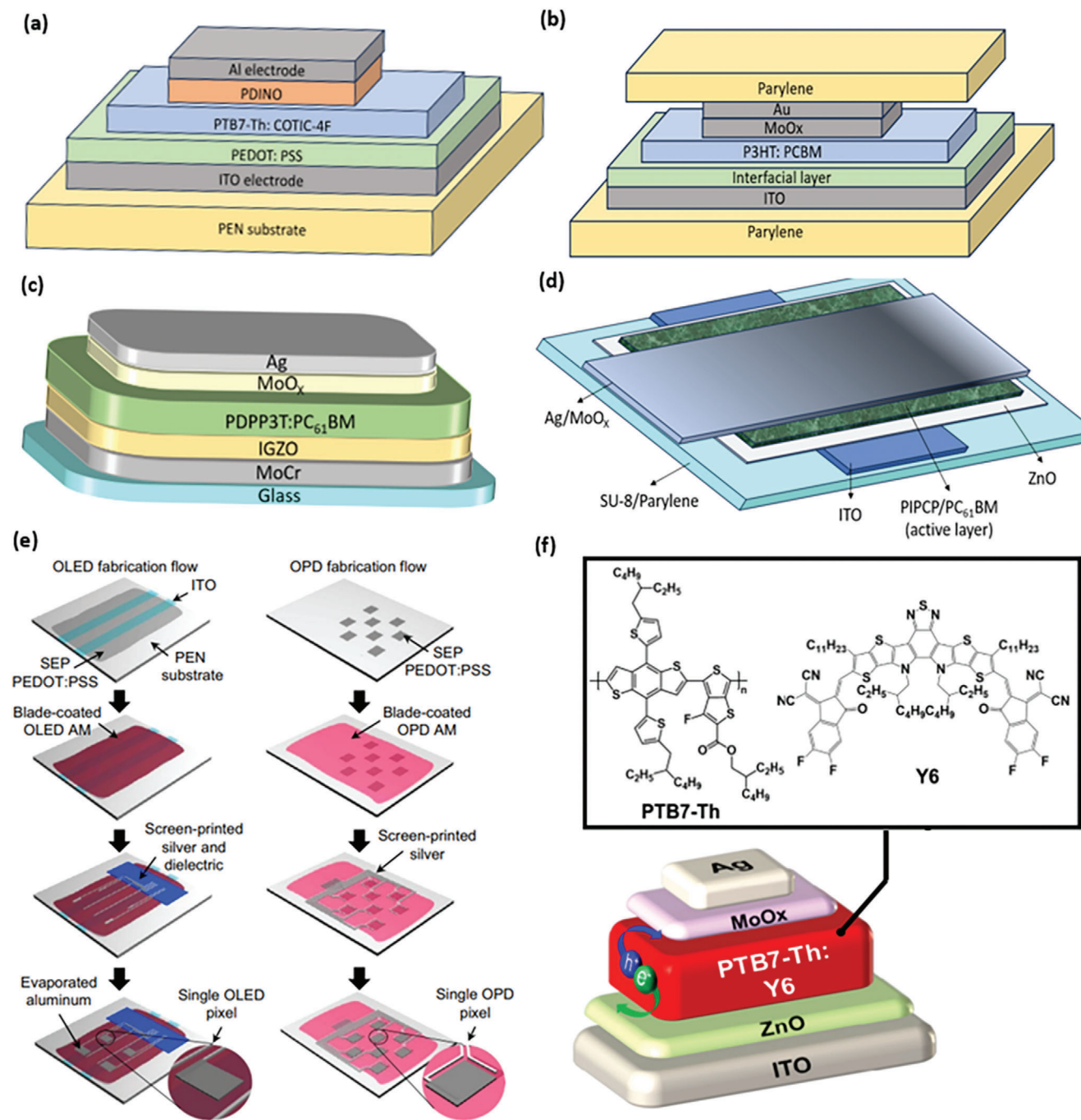


Figure 7. Illustration of the developed PPG organic photodetector fabricated by a) Simoes et al.;^[26] b) Yokota et al.;^[48] c) Simone et al.;^[49] d) Park et al.;^[50] e) Khan et al.^[51] (Reproduced under terms of CC-BY license.^[51] Copyright 2018, the Authors, published by PNAS); f) Eun et al.^[47] (Reproduced under terms of CC-BY license.^[47] Copyright 2022, The Authors, published by iScience).

Xu et al.^[52] developed a flexible PPG sensor to measure heart rate and BP using a photodetector with an active layer of DPP-DTT: PCBM and a commercial NIR LED. The fabrication process of the photodetector is illustrated in **Figure 9**. Si wafer was used as the sacrificial layer, and the substrate was a thick layer of polyimide. The gate electrode and the source/drain electrode, on the top and bottom of the $\text{Al}_2\text{O}_3/\text{SiO}_2$ gate dielectric, were made of

gold (Au). The whole photodetector was finally encapsulated with a layer of polytetrafluoroethylene and parylene subsequently. The fabricated PPG device had low power consumption and high responsivity due to the bulk heterojunction active layer and the gate dielectric structure. The heart rate and BP of a human subject were measured from the left index finger using the reflection mode. The obtained values were validated by comparing them

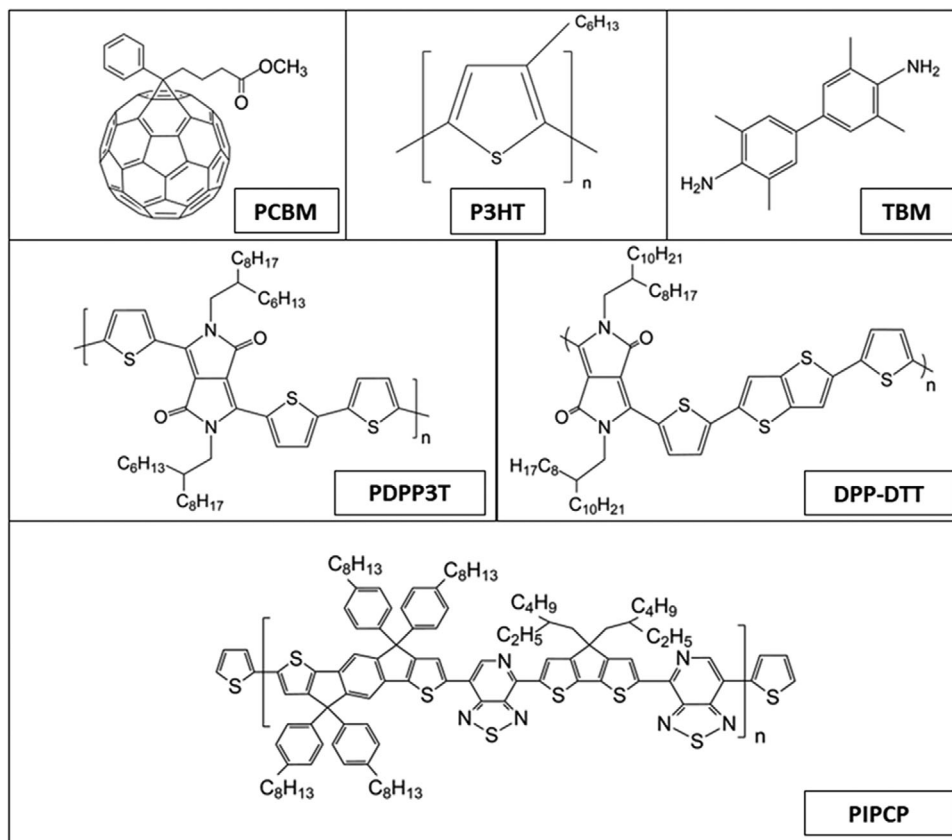


Figure 8. The chemical structures of PCBM, P3HT, PDPP3T, PIPCP, TMB, and DPP-DTT polymers.

with the corresponding values obtained from a commercial PPG sensor working in reflection mode.

3.1.3. Nanomaterials

Materials with at least one dimension less than 100 nm are classified as nanomaterials, gaining worldwide attention across all scientific fields due to their unique optical, electrical, mechanical, and thermal properties. This section will summarize different nanomaterials used in the fabrication of PPG devices.

Graphene and PbS QDs: Graphene is a 2D single layer of carbons arranged in a closely packed honeycomb struc-

ture. Owing to its high surface to volume ratio, outstanding electrical conductivity (1732 S/m), excellent mechanical strength (≈ 125 GPa), good flexibility, and other exceptional optical properties, graphene has been using in numerous optoelectronic devices.^[70] On the other hand, PbS QD is an inorganic semiconductor material with a band gap of 1.2 eV,^[71] high surface activities, chemical inertness, good tunable emission wavelength photoluminescence properties, and exceptional stability due to edge effects and quantum confinement. These properties make PbS QD a suitable candidate for many thermoelectrical and optoelectronic devices.

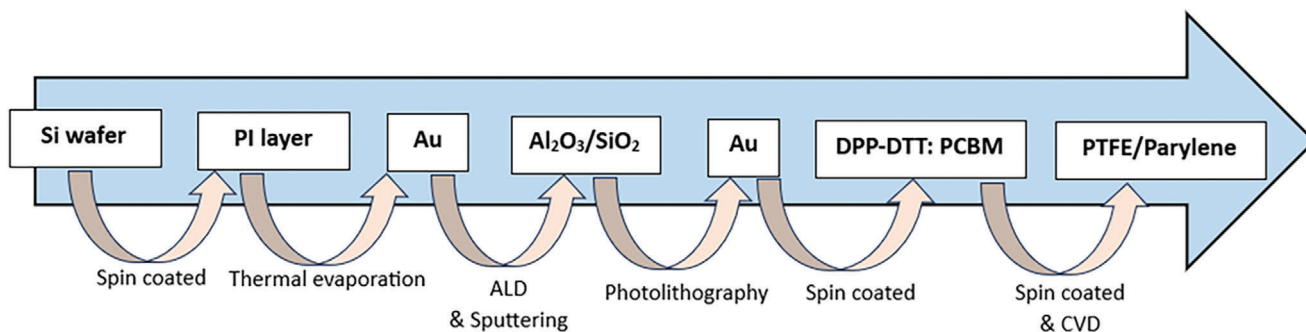


Figure 9. Illustration of steps followed by Xu et al.^[52] for the fabrication of the photodetector. (ALD: Atomic layer deposition, CVD: Chemical vapor deposition).

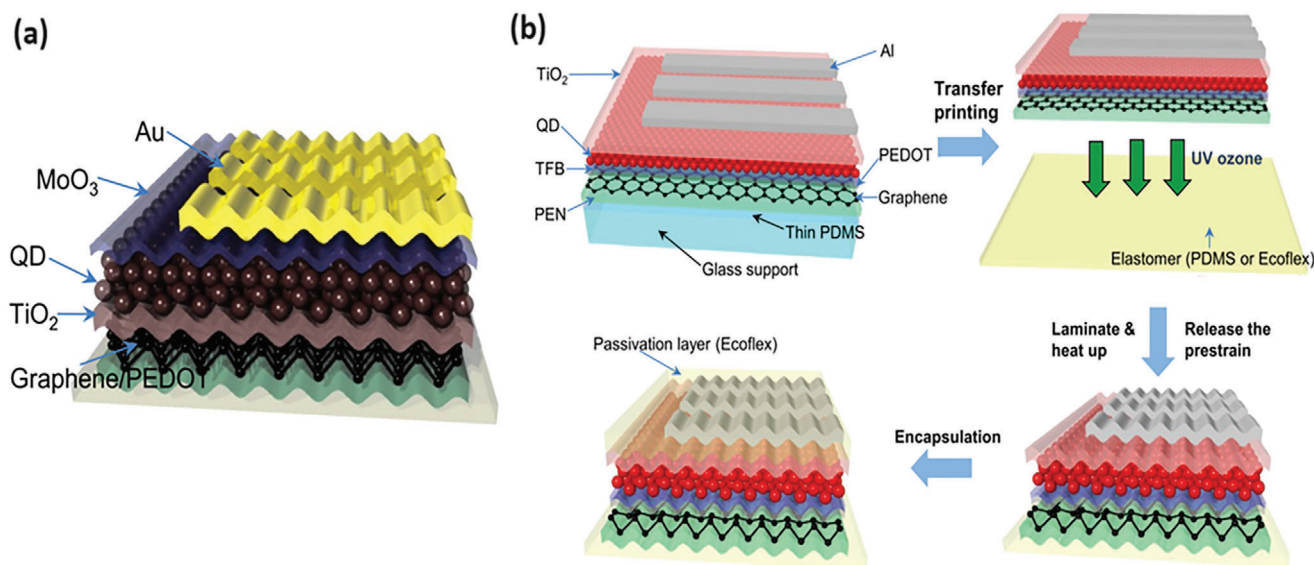


Figure 10. Steps followed by Kim et al.^[53] in the fabrication of a) photodetector b) QD LED (Reprinted with permission.^[53] Copyright 2017, American Chemical Society).

Kim et al.^[53] fabricated an optoelectronic device comprising QD-based LEDs and a PbS QD-based photodetector. **Figure 10a** illustrates the workflow in the fabrication of QD-photodetector. After fabricating the QD-LED and the QD-photodetector, these were printed onto a pre-strained Ecoflex. Then, the pre-strained Ecoflex was released to form a regular wavystructured PPG device. The fabricated device was waterproof, ultrathin, stretchable, and worked on the transmission mode. It measured the pulse rate from the forefinger of one male subject and the readings were compared with the expected values of a healthy human.

Polat et al.^[54] developed PPG devices composed of graphene and PbS QDs photodetectors. They fabricated three photodetectors on polyethylene terephthalate (PET), PEN, and polyimide. Initially, chemical vapor-deposited graphene was transferred onto the substrates. Then, a photosensitive layer of PbS QDs was spin-coated on the graphene. Finally, the entire device was laminated by a PET cap to avoid mechanical damage caused by skin interaction. The photosensitivity and the mechanical robustness of the three devices were tested to compare the mechanical flexibility and light sensitivity. The fabricated devices were used to measure the heart rate, blood oxygen saturation, respiratory rate, and UV skin exposure. The devices were operated in a reflectance mode using a green LED and transmission mode using ambient light. The measured readings were validated with a clinical setting state-of-art PPG sensor, showing high responsiveness and mechanical stability.

ZnO Nanomaterials: ZnO nanomaterial is a wurtzite n-type semiconductor material with a high exciton binding energy of 60 meV and a wide band gap of 3.37 eV.^[72] Because of these properties, along with a high-surface-to-volume ratio, ZnO nanomaterials have garnered extensive research interest for their potential application in piezoelectric sensors, mechanical actuators, nanogenerators, solar cells, and photodetectors.

Lee et al.^[55] fabricated fiber-based QD LEDs and a fiber-based organic photodetector using ZnO NPs to develop a pulse oximeter. The different steps in the construction of the photodetector

are shown in **Figure 12a,b**. Fabricated LEDs and the photodetector were encapsulated and slit using inorganic/organic nano laminated-based thin films with Al₂O₃/ZnO and SiO₂ composite polymer to improve the optical characteristics and the reliability of the device. The reliability of the device was investigated using a bending test (8 mm radius of curvature) and an operating lifetime test (stable 8000 h). The developed PPG device consisted of red and green LEDs functioning in reflection mode to measure the blood oxygen saturation in a single human subject. The obtained values were validated with a commercial pulse oximetry.

3.1.4. Hybrid Materials

Recently, several studies have been conducted in the field of PPG where the photodetectors were composed of a combination or a blend of different types of materials. Here, the term “hybrid materials” refers to the blend or combination of different materials to enhance the performance of photodetectors. Most of the PPG devices fabricated by these materials showed outstanding characteristics compared to conventional PPG devices. This section will briefly discuss the hybrid materials and fabrication processes used in PPG devices that incorporate combinations of organic, inorganic, nanomaterials, or their combinations.

Indium Gallium Zinc Oxide (IGZO) and Diketopyrrolopyrrole (DPP) Polymer: IGZO is an amorphous n-type semiconducting material with high transparency and good field effect mobility. It has a large energy band gap of 3.05 eV and a good electron mobility of 10 cm² V⁻¹ s⁻¹.^[73] IGZO can be prepared with ease using a simple deposition technique resulting in large area uniformity. DPP is an organic p-type semiconducting polymer that is widely used in field effect transistors, high-quality pigments, fluorescence imaging, and bulk heterojunction solar cells.^[74]

Kang et al.^[56] developed a skin-conformable PPG sensor using IGZO/DPP hybrid material as the active layer for measuring the heart rate and blood oxygen saturation. The structure of the

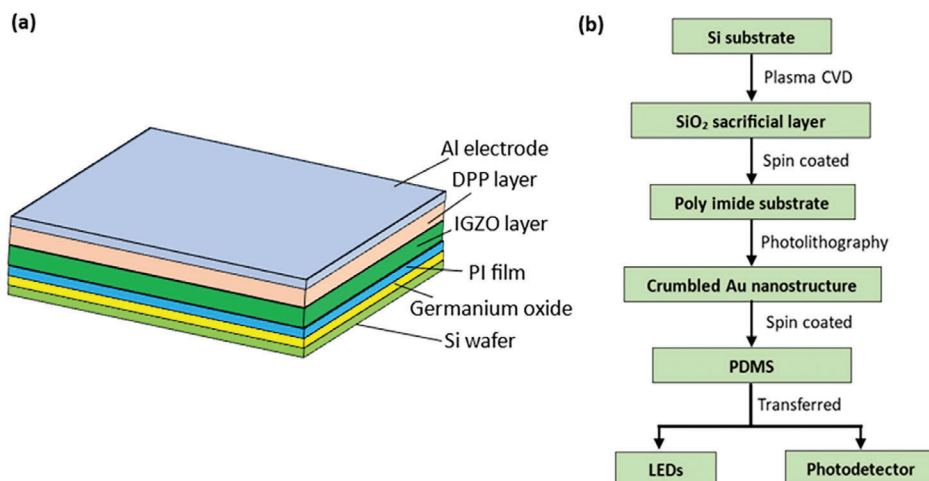


Figure 11. a) Structure of the hybrid phototransistor by Kang et al.^[56] b) Illustration of fabrication steps followed by Chen et al.^{[57].an}

fabricated hybrid phototransistor is shown in **Figure 11a**. Boron-doped Si wafers and germanium oxide were used as the sacrificial substrate for the active layer and aluminum was used as the electrodes. The polyimide film was deposited using spin coating and cured on the Si substrate. A layer of each of IGZO and DPP was spin-coated onto the polyimide substrate one after the other sequentially. After the lift-off process, the entire device was transferred to an adhesive PDMS substrate.

The fabricated sensor consisted of two LEDs (red and NIR) along with two hybrid phototransistors. Operating in the reflection mode, the device measured the heart rate and oxygen saturation during rest and walking, acquiring measurements from the index finger of 10 human subjects. The accuracy of the acquired data was confirmed through comparison with an off-the-shelf PPG device.

Gold Nanostructure on PDMS: Au nanomaterials exhibit many attractive optical, electrical, and catalytic properties. They offer size-tunable luminescence and plasmonic color properties rendering them desirable for applications in bio-imaging, bio-analyses, and optical devices.^[75] PDMS are a group of organic Si-based polymers commonly known for their unusual rheological properties. They are generally used as a substrate in many PPG devices and the manufacturing of contact lenses as they are non-toxic, non-flammable, inert, hydrophobic, and optically transparent.^[76]

Chen et al.^[57] developed an optoelectronic device using a triboelectric nanogenerator made from crumpled Au nanostructure and PDMS. Ultrathin LEDs and photodetectors were fabricated to a self-powered PPG device that can measure the blood oxygen saturation and pulse rate from the thumbnail of a human subject. The fabrication process of the triboelectric nanogenerator and the PPG device is illustrated in **Figure 11b**. Once the LEDs and the photodetectors were transferred to the crumpled Au layer, liquid PDMS was spin-coated onto it and cured to form a protective enclosure. The SiO₂ sacrificial layer was then etched with hydrofluoric acid. The nanogenerators harvest and store energy from the body motion (finger bending) and supply it to the LEDs and other signal-processing parts to make the device battery-free. When there is a body motion where the device is attached, the Au

layer and the PDMS layer come in contact with each other. As a result, charges are developed on the contact surface. When the force is released, the electrons will flow from the upper to lower electrodes and therefore the layers return to their initial states. Conversely, when pressure is applied to the PPG device, the electrons flow in the opposite direction, generating power for operating the device. The device worked in reflection mode using a red LED and an IR LED to measure the blood oxygen saturation. Validation of the collected data was undertaken using a commercially accessible oximeter.

3.2. Materials used in the Fabrication of LEDs and Interconnects of PPG Devices

Majority of the PPG sensors studied herewith used commercial LEDs. Out of these, Kim et al.,^[44] Li et al.,^[45] and Xu et al.^[52] used LEDs comprising AlGaAs and/or AlGaInP. Other studies did not mention about the material of the LED they have used. However, Yokota et al.,^[48] Khan et al.,^[51] Kim et al.,^[53] and Lee et al.^[55] fabricated their own LEDs for their PPG devices.

Yokota et al.^[48] fabricated polymer-based LEDs on parylene films and ITO, sputtered on the film as transparent electrodes. Then, a hole injection layer and an interlayer were spin-coated on top of it, followed by spin coating of an active emissive polymer layer consisting of fluorenes, phenylenes, and other condensed aromatic polymers. NaF/Al cathode was deposited on top of the emissive layer. After the fabrication of the polymer LEDs, a passivation layer consisting of 5 alternating inorganic SiON and organic parylene layers were assembled using plasma-enhanced chemical vapor deposition to improve the stability of the device. They fabricated both the light source (blue, green, and red) and the photodetector using polymers. In another example, Khan et al.^[51] fabricated organic LEDs on a PEN substrate patterned with ITO (**Figure 7e**). After making the surface hydrophobic, the substrate was patterned by using plasma for selective etching of the hydrophobic layer. Then, an interlayer of PEDOT: PSS and the active emissive layer were blade coated subsequently on the substrate. On top of it, dielectric and silver traces were screen

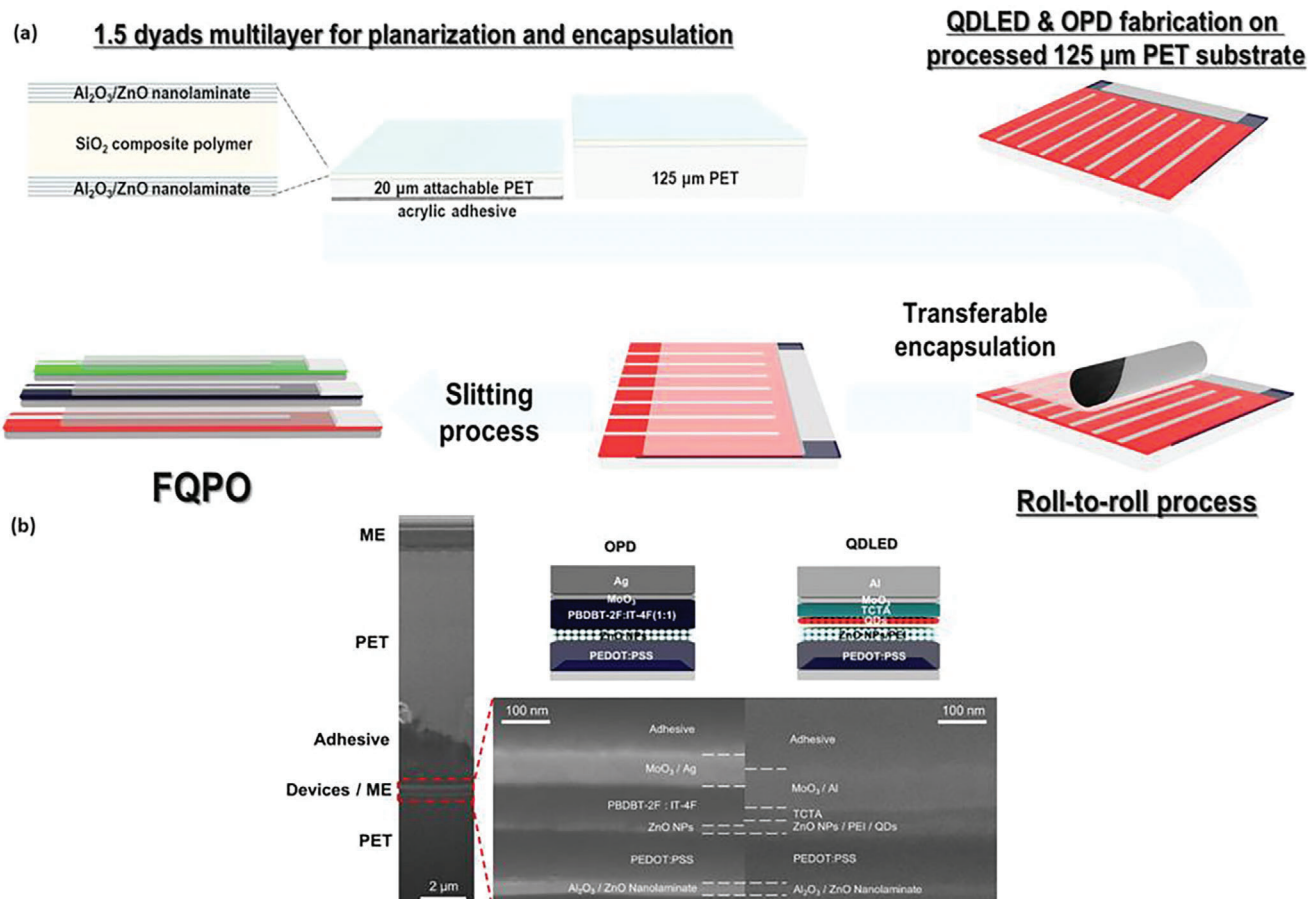


Figure 12. a) Fabrication processes of the photodetector and the LED followed by Lee et al.^[55] b) Structure of the photodetector and the LED of Lee et al.^[55] (Reproduced under terms of CC-BY license.^[55] Copyright 2023, The Authors, published by npj Flexible Electronics).

printed. Silver traces were used to connect the electrodes of each array unit, whereas dielectric traces were used to prevent shorts between the ITO and the silver traces. Finally, a layer of calcium and aluminum was deposited using thermal evaporation to form the cathode and each developed array was then encapsulated in UV-curable epoxy and a plastic film. Kim et al.^[53] used a combination of CdSe, CdS, and ZnS (core/shell/shell) QDs for the fabrication of red LED, whereas a combination of CdSe and ZnS QDs was used for developing green and blue LEDs. Figure 10b illustrates the workflow in the fabrication of QD-LED. TiO₂ layers and poly[(9,9-dioctylfluorenyl-2,7-diyl)-co-(4,4'-(N-(4-s-butylphenyl)) diphenylamine)] (TFB) were used as the electron and hole transport layers respectively in the QD-LED. The fabricated LEDs were validated by comparing the readings obtained by using a commercial ITO-based LED. Lee et al.^[55] fabricated fiber-based QD LEDs using ZnO NPs to develop a pulse oximeter. The steps in the construction of the LEDs are illustrated in Figure 12a and b.

Electronics is a well-established engineering field and therefore different materials with good properties have been used in the fabrication of electronic circuits for diverse equipment. PPG devices use electronic circuits and inter-connects to aid supply power, transfer, and process electrical signals from and to photodetectors. The commonest materi-

als used in the circuits of PPG device are Au, copper, and silver. Li et al.,^[45] Eun et al.,^[47] Park et al.,^[50] Polat et al.,^[54] and Chen et al.^[57] used Au coils/wires for electronic circuits of their PPG devices. Kim et al.^[44] and Kim et al.^[46] used Cu wires, whereas Khan et al.^[51] used silver traces in the electronic circuits of their PPG devices. Kim et al.^[43] used a combination of Au and chromium in the electronic circuits. Other studies, however, did not mention about the material used in the electronic circuits of their PPG sensors. Despite the higher cost of Au in comparison with Cu and Ag, it excels in terms of electrical conductivity, resistance to corrosion, and ease of manipulation. Therefore, most of the PPG devices use Au in the electronic circuits.

4. Technical Details in Physiological Measurement

Heart rate and blood oxygen saturation are the two prevailing physiological parameters monitoring with PPG sensors. Apart from these parameters, recent PPG sensors also measure physiological parameters like respiration rate, mental stress, UV exposure, artery stiffness, and skin color detection by adopting new designs and modifying technical details such as the light source, mode of operation, and measurement sites.

Table 2. Physiological parameters measured by the studied PPG sensors.

PPG-derived Physiological Parameters	Definition	References of the Measured PPG Sensors
Heart rate	The number of times heart beats per minute	[26,27,43–47,49,50,52–54,56,57]
Blood oxygen saturation	The ratio of oxygen bounded hemoglobin to the non-oxygen bounded hemoglobin in the blood	[26,44–46,48,49,51,54–57]
UV exposure	The amount of ultraviolet radiation incident on a subject per unit area	[44,54]
Respiration rate	The number of breaths a subject takes per minute	[54]
Skin color detection	Detection of the skin color and its changes in pathological conditions	[44]
Artery stiffness	The rigidity of the arterial wall, often described by the relation between intra-arterial pressure and lumen cross-sectional area (or diameter). ^[77]	[49]

4.1. PPG-Derived Physiological Parameters: Measurement and Validation

Table 2 lists the PPG-derived physiological parameters in the reviewed studies. Heart rate and blood oxygen saturation are the two most common PPG-derived physiological parameters. Most studies measured and validated human heart rate except for Yokota et al.,^[48] Khan et al.,^[51] and Lee et al.^[55] Blood oxygen saturation readings were taken by most of the inorganic and nanomaterial-based PPG devices, but some organic material-based PPG devices did not measure this. Reading of blood oxygen saturation of a subject requires a minimum of two LEDs with different wavelengths, and additional electronics to process the data.^[9] Generally, PPG devices using organic materials are more complex in structure than inorganic counterparts, which may add difficulties to oxygen saturation measurement.

Apart from the heart rate and blood oxygen saturation, readings of other physiological parameters like UV exposure, skin color detection, artery stiffness, quality of blood circulation, and respiration rate were also done by some of the reviewed PPG devices as shown in Table 2. A modified Si-based PPG device fabricated by Kim et al.^[44] measured ultraviolet exposure and color detection of human skin apart from the heart rate and blood oxygen saturation. Similarly, the PPG device fabricated by Polat et al.^[54] using PbS QDs and graphene is also able to detect skin color, ultraviolet exposure, heart rate, and blood oxygen saturation. In addition to these, they also measured the respiration rate of the human subject by in-depth processing and analyzing the received PPG signals. The PPG sensor fabricated by Simone et al.^[49] using PCBM and PDPP3T also measured artery stiffness apart from heart rate and blood oxygen saturation. The measurement of artery stiffness was achieved by evaluating the second derivative of the PPG signal and the time delay between the systolic and diastolic peaks.

All the reviewed PPG devices took different physiological readings from human subjects. The majority of the researchers validated the obtained readings from their devices by comparing the values measured under the same conditions from a state-of-art pulse oximeter or PPG sensor. In contrast, Kim et al.,^[43] Park et al.,^[50] and Eun et al.^[47] validated the readings of their PPG devices by comparing them with the standard values of a healthy human by assuming the subject has no health issues. In another example, Li et al.^[45] validated the readings of their PPG devices

by taking and comparing the readings from different locations of the tested subjects.

4.2. Mode of Operation, Light Sources, Measurement Sites, Testing and Validation of Mechanical Properties

The mode of operation of PPG devices depends on the wavelength of the light sources regardless of the materials used for the fabrication. Out of 17 studied PPG devices, three studies adopted transmission of operation,^[26,47,53] one study used both modes of operation,^[54] two studies did not mention the mode of operation for their devices,^[27,50] and the remaining studies adopted reflection mode of operation. The light source used by the PPG sensors reviewed in this paper is illustrated in Figure 13. Light sources with higher wavelengths (deep penetration) are required to achieve a transmission mode of operation. Therefore, red or infrared-based light sources are preferably used in these PPG devices. On the other hand, for reflection mode PPG devices, blue, green, red, or infrared light sources are used leading to good PPG signals. The light source and the photodetector are placed on the same side, making the device more compact and reliable. However, such PPG devices are more exposed to noise than the transmission mode-based PPG devices.

To get accurate readings of various physiological parameters like heart rate and blood oxygen saturation, the measuring sites should have sufficient blood vessels, arteries, and veins as well as soft tissues rather than hard tissues and bones. Fingers, nails, forearms, wrists, forehead, and earlobes were the commonest measurement sites of PPG signals.^[78] Figure 14 shows the measurement sites used in the reviewed studies. More than 70% of studied PPG devices used finger/fingertip which included rich microcirculation and small arteries and veins. In addition, the unique geometry of finger enables both transmission and reflection modes in PPG sensing. Another advantage of using fingers/fingertips as the measuring sites is that the PPG device can adhere to the skin reliably and hence cause less discomfort to the subjects. Whereas, the finger is flexible, with much motion artifact especially in daily monitoring. The wrist and forearm provide more ease and comfort for PPG sensing,^[79,80] but are also sensitive to motion artefacts.^[81] Forehead, earlobes, and nails might be less prone to motion artifacts.^[43,82,83] However, adhering PPG devices to these sites is difficult and may cause discomfort.^[84]

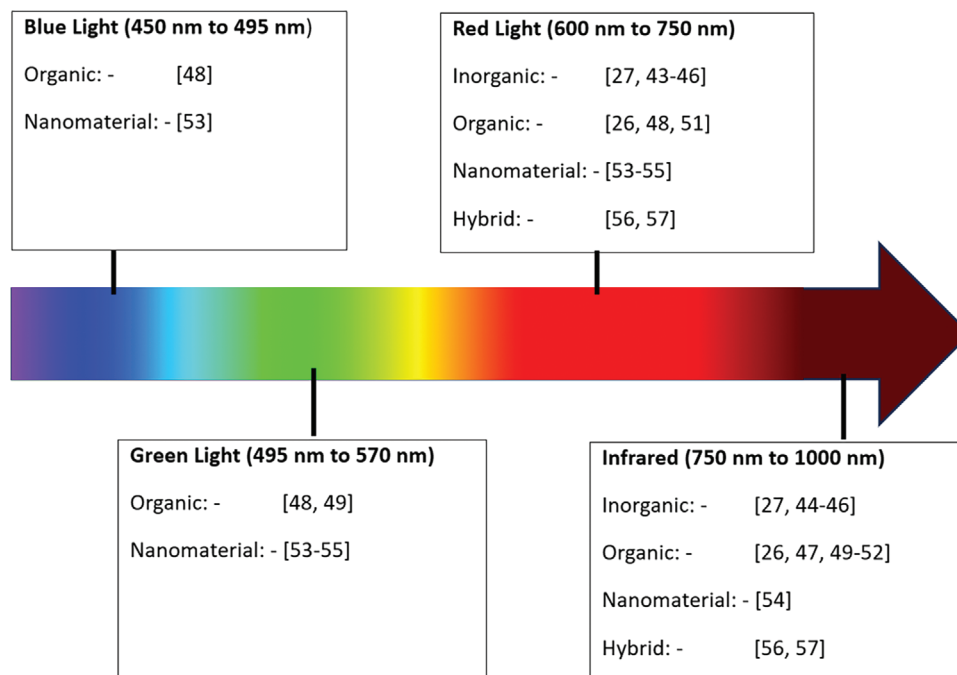


Figure 13. Light wavelength involved in various PPG devices.

Testing's and validations of mechanical properties like flexibility, strength, and structure of the materials can ensure the applicability and reliability of PPG devices. Table 3 summarizes details of the mechanical tests in the reviewed studies. The mechanical properties of the PPG devices largely depend on the materials especially the substrate.^[88] The majority of them have used the cyclic bending test, as when PPG devices are worn, these devices experience a large bending force in comparison with other types of forces. Uni-axial testing is also a good mechanical validation test to measure the stretchability and flexibility of the fabricated PPG sensors. Simoes et al.^[26] and Li et al.^[45] performed tensile tests for their PPG devices. A limitation of tensile test is that the device/specimen to be tested should be within certain ranges of thickness, width, and length so it can be fixed firmly. Scanning electron microscopy (SEM) and transmission electron microscopy (TEM) tests are usually performed to study the structure, compositions, and defects of nano/micro materials used for PPG devices. SEM and TEM can reveal materials' structural and mechanical properties on a microscopic level but are expensive. Finite element analysis/ finite element method (FEA/FEM) are in silico computational simulations that can estimate the strain, stress, and displacement in different loads. FEA/FEM is a low-cost approach that can provide reference for the optimization of the sensor geometry to suit different application scenarios before any in vitro experiment.

5. Perspectives and Conclusions

The advantages and limitations of the materials in recent PPG sensors are summarized in Table 4. Organic, nanomaterials or hybrid materials can enhance the flexibility and stretchability of the device compared to inorganic materials. PPG sensors comprising inorganic materials like Si and GaAs, have a simple de-

sign and can make the device to be ultrathin or miniaturized. This also enables the integration of PPG device with other modules to add more functional features like battery-free operation. But such inorganic devices are more sensitive to motion artifacts. There is a relative scarcity of research on the fabrication of PPG devices using nanomaterials and hybrid materials. For many advanced materials in different types, complex fabrication process and high costs are common limitation for mass production.

Overall, compared with parallel studies in other wearable techniques, there are limited advanced materials in PPG devices. Semiconducting organic materials like PCBM, PTB7-Th, PIPCP, have been proposed as alternatives to inorganic materials to overcome their drawbacks. Various nanomaterials and hybrid materials have been investigated in many fields like electronics and computing industries,^[89,90] medical equipment,^[91] transportation,^[92] and solar cells.^[93] Some eco-friendly, self-repairing, and energy-harvesting materials are also to be explored in PPG sensing.^[94-96]

Toward next-generation wearable PPG sensors, miniaturization with super-thin structure (i.e., tattoo sensor), reliable skin adhesion, integrated multiwavelength sensing, as well as opacity and transparency for different components are the major challenges. In addition, the high sensitivity and robustness against motion artefact are to be considered in a balanced perspective. The unmet challenges for large-scale healthcare applications include low-cost materials, simplified fabrication process, and standardized integration with other devices via internet-of-things (IoT).^[97-99] These challenges introduce higher requirements for optic and electronic sensitivities, flexibility, stretchability, skin adhesion, etc.

Advanced materials could enhance the quality of PPG signals,^[100] reduce the complexity of preprocessing,^[101] and enable the measurement of multiple physiological parameters

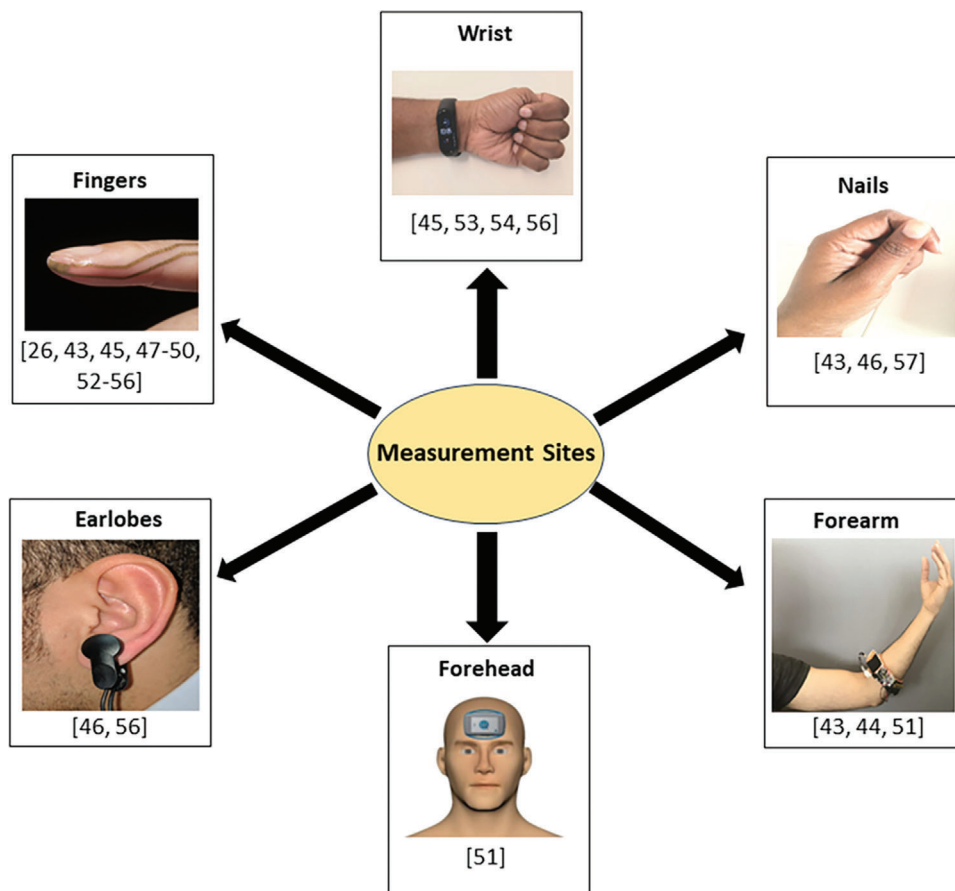


Figure 14. Various measurement sites used by studied PPG devices (adapted from [83,85–87]) (Earlobe- Reproduced under terms of the CC-BY license.[83] Copyright 2018, The Authors, published by MDPI; Forearm- Reproduced under terms of the CC-BY license.[85] Copyright 2020, The Authors, published by Frontiers; Forehead- Reproduced under terms of the CC-BY license.[87] Copyright 2022, The Authors, published by BMJ; Fingers- Reproduced with permission.[86] Copyright 2021, Elsevier).

Table 3. Various mechanical tests conducted by the studied PPG devices.

Name of the Mechanical Test	Objectives	Type of Materials	References of the Tested PPG Sensors
Cyclic bending test	To measure the fatigue strength of the device/material under repeated bending.	All types	[26,43,48,50,55]
Tensile test	To identify the tensile strength and how the device/material can be stretched before it fails.	All types of materials having enough thickness, width, and length	[26,45]
Finite element analysis/ finite element method (FEA/FEM)	A software and mathematical-based test to simulate how device/material will react to different forces, vibration, heat, and/or other physical effects.	All types of materials with known standard properties	[44,45]
Scanning electron microscopy (SEM)	An instrumental test to examine and analyze the structure, compositions, and defects of nano/micro materials through images.	All types of nano/micro materials	[45,53,56]
Transmission electron microscopy (TEM)	An instrumental test to examine and analyze the structure, compositions, and defects of nano/micro materials through images.	All types of nano/micro materials	[53]
Endurance test	To measure the performance of the device when using constantly.	All types	[57]
Compression test	To study the device/material's response when it is compressed.	All types of materials having enough thickness, width, and length	[48,50]

Table 4. Advantages and limitations of different types of materials used in PPG sensors (The materials used by each reference can be identified by referencing to Table 1).

	Inorganic	Organic	Nanomaterials	Hybrid Materials
Advantages				
Mechanical flexibility	[43,45]	[26,47,48,50,51]	[53–55]	[56,57]
Conformability with skin	[43–45]	[48,50]		[56]
Miniaturized/ultrathin	[27,45,46]	[50]		
Resistance to motion artifacts	[27,46]	[47]	[53,55]	
Suppression of dark current		[49]		[56]
Stretchability	[45]	[48]	[53,55]	
Battery-free operation	[44,46]		[54]	[57]
Disadvantages				
Noise due to motion artifacts	[43,44]	[26]		
Complex design/process	[44–46]	[48,49,51]	[53,54]	[56,57]
High dark current		[26,50]		
Bulky	[27]			

including respiratory rate, heart rate, and their variabilities via demodulation,^[102] providing new potentials for early diagnosis of cardiovascular, respiratory, neurological, and metabolic diseases.^[103–105]

The future focus of advanced materials in PPG sensing will be on cutting down the cost, simplifying the fabrication processes, as well as exploring more advanced and hybrid materials. These endeavors in material sciences may achieve reliable, accurate, and multiwavelength PPG sensing with robustness against noises and applicability in different cohorts and scenarios. Applications of nanomaterials like carbon nanotubes, Si NPs, graphene, titanium dioxide NPs, Au NPs, silver NPs, and ZnO NPs have been investigated in flexible electronics with high computational capacity,^[106] advanced medical devices including miniaturized surgery robot,^[107] biodegradable sensors,^[108] energy harvesting.^[109] The results of these investigations proved that nanomaterials could enhance the properties and performance of wearable sensors compared with their counterparts inorganic or organic materials. Therefore, the applicability of these nanomaterials can also be investigated in the fabrication of PPG sensors. Materials with high biocompatibility and flexibility can enable the exploration for sensor miniaturization and long-term daily monitoring.^[110] The potential to integrate PPG sensors with other devices such as electrocardiograms, blood glucose meters, and electronic thermometers is a cutting-edge technology for comprehensive evaluation of physiological status. The large-scale validation of proposed PPG sensors is also necessary for healthcare applications.

The development of wearable PPG sensors has been accelerating over the last decade with the applications extended to various clinical and healthcare scenarios. Advanced materials including organic, inorganic, nanomaterials, and hybrid materials have been applied in different components of PPG sensors, especially the photodetector, to improve the photoelectric and biomechanical properties. Many physiological parameters and conditions are detectable using the PPG sensors enhanced by advanced materials, while many sensors need further large-scale validation. In future research, more advanced materials can be explored toward real-world healthcare applications.

Acknowledgements

The authors were grateful to Coventry University and Institute of Materials Research and Engineering, A*STAR (Agency for Science, Technology and Research) for the support and facilities provided for the completion of this work. Horizontal Technology Coordinating Office Seed Fund, Singapore (No. C231218001).

Conflict of Interest

The authors declare no conflict of interest.

Keywords

inorganic materials, nanomaterials, organic materials, photodetectors, photoplethysmography, wearable sensors

Received: November 7, 2023

Revised: January 26, 2024

Published online:

- [1] L. Menghini, E. Gianfranchi, N. Cellini, E. Patron, M. Tagliabue, M. Sarlo, *Psychophysiology* **2019**, *56*, 13441.
- [2] S. Mondal, N. Zehra, A. Choudhury, P. K. Iyer, *ACS Appl. Bio Mater.* **2020**, *4*, 47.
- [3] T. Chaudhuri, Y. C. Soh, H. Li, L. Xie, *Build. Environ.* **2020**, *170*, 106615.
- [4] Y. Huang, L. Zhao, M. Cai, J. Zhu, L. Wang, X. Chen, Y. Zeng, L. Zhang, J. Shi, C. F. Guo, *Adv. Healthcare Mater.* **2023**, 2301838.
- [5] J. Chen, M. Abbod, J.-S. Shieh, *Sensors* **2021**, *21*, 1030.
- [6] G. Yang, W. Tan, H. Jin, T. Zhao, L. Tu, *Cluster Computing* **2019**, *22*, 3021.
- [7] S. Chen, J. Qi, S. Fan, Z. Qiao, J. C. Yeo, C. T. Lim, *Adv. Healthcare Mater.* **2021**, *10*, 2100116.
- [8] C. Yang, D. Zhang, D. Wang, X. Chen, H. Luan, *J. Mater. Chem. C* **2022**, *10*, 7076.
- [9] M. A. Almarshad, M. S. Islam, S. Al-Ahmadi, A. S. Bahammam, *Healthcare* **2022**, *10*, 547.
- [10] H. Liu, J. Allen, D. Zheng, F. Chen, *Physiol. Measure.* **2019**, *40*, 07TR01.

- [11] S. Gedam, S. Paul, *11th International Conference on Computing, Communication and Networking Technologies (ICCCNT) 2020*, 1.
- [12] M. Kebe, R. Gadhafi, B. Mohammad, M. Sanduleanu, H. Saleh, M. Al-Qutayri, *Sensors* **2020**, *20*, 1454.
- [13] N. Huang, M. Zhou, D. Bian, P. Mehta, M. Shah, K. S. Rajput, N. Selvaraj, *43rd Annual International Conference of the IEEE Engineering in Medicine & Biology Society (EMBC) 2021*, 7470.
- [14] S. Gedam, S. Paul, *IEEE Access* **2021**, *9*, 84045.
- [15] W. Wu, L. Wang, G. Shen, *J. Mater. Chem. C* **2023**, *11*, 97.
- [16] P. H. Charlton, V. Marozas, *Photoplethysmography* **2022**, 401.
- [17] I. Lee, N. Park, H. Lee, C. Hwang, J. H. Kim, S. Park, *Appl. Sci.* **2021**, *11*, 2313.
- [18] W. Sun, Z. Guo, Z. Yang, Y. Wu, W. Lan, Y. Liao, X. Wu, Y. Liu, *Sensors* **2022**, *22*, 7784.
- [19] J. Azar, A. Makhoul, R. Couturier, J. Demerjian, *Computers & Electrical Engineering* **2021**, *92*, 107065.
- [20] S. Puranik, A. W. Morales, *IEEE Transactions on Consumer Electronics* **2019**, *66*, 69.
- [21] G. Biagetti, P. Crippa, L. Falaschetti, S. Orcioni, C. Turchetti, *Biomedical Signal Processing and Control* **2019**, *52*, 293.
- [22] B. Mishra, N. S. Nirala, *IEEE International Conference for Innovation in Technology (INOCON) 2020*, 1.
- [23] D. Luguern, Y. Benezeth, V. Moser, L. A. Dunbar, F. Braun, A. Lemkaddem, K. Nakamura, R. Gomez, J. Dubois, *14th International Symposium on Medical Information Communication Technology (IS-MICT) 2020*, 1.
- [24] G. H. Lee, H. Kang, J. W. Chung, Y. Lee, H. Yoo, S. Jeong, H. Cho, J.-Y. Kim, S.-G. Kang, J. Y. Jung, *Sci. Adv.* **2022**, *8*, eabm3622.
- [25] X. Peng, K. Dong, C. Ye, Y. Jiang, S. Zhai, R. Cheng, D. Liu, X. Gao, J. Wang, Z. L. Wang, *Sci. Adv.* **2020**, *6*, eaba9624.
- [26] J. Simões, T. Dong, Z. Yang, *Adv. Mater. Interfaces* **2022**, *9*, 2101897.
- [27] P. Fallica, D. Lena, F. Rundo, S. Conoci, *Sensors and Microsystems* **2021**, 314.
- [28] J. V. Dcosta, D. Ochoa, S. Sanaur, *Adv. Sci.* **2023**, *10*, 2302752.
- [29] H. Anabestani, S. Nabavi, S. Bhadra, *Nanomaterials* **2022**, *12*, 3775.
- [30] T. Tamura, Y. Maeda, M. Sekine, M. Yoshida, *Electronics* **2014**, *3*, 282.
- [31] S. Zhang, T. Zhang, Z. Liu, J. Wang, J. Xu, K. Chen, L. Yu, *Adv. Funct. Mater.* **2022**, *32*, 2205462.
- [32] H. Ren, J. D. Chen, Y. Q. Li, J. X. Tang, *Adv. Sci.* **2021**, *8*, 2002418.
- [33] Z. Zhao, C. Xu, L. Niu, X. Zhang, F. Zhang, *Laser Photonics Rev.* **2020**, *14*, 2000262.
- [34] X.-R. Zhang, J.-Z. Jiang, B.-G. Feng, H.-F. Song, L. Shen, *J. Mater. Chem. C* **2023**, *11*, 12453.
- [35] L. Shi, Q. Liang, W. Wang, Y. Zhang, G. Li, T. Ji, Y. Hao, Y. Cui, *Nanomaterials* **2018**, *8*, 713.
- [36] L. Xie, Z. Zhang, Q. Wu, Z. Gao, G. Mi, R. Wang, H.-B. Sun, Y. Zhao, Y. Du, *Nanoscale* **2023**, *15*, 405.
- [37] S. Hussain, J. Chae, K. Akbar, D. Vikraman, L. Truong, B. A. Naqvi, Y. Abbas, H.-S. Kim, S.-H. Chun, G. Kim, *Nanomaterials* **2019**, *9*, 1460.
- [38] F. Zacharatos, I. Theodorakos, P. Karvounis, S. Tuohy, N. Braz, S. Melamed, A. Kabla, F. De La Vega, K. Andritsos, A. HatziaPOSTOLU, *Materials* **2018**, *11*, 2142.
- [39] M. A. Butt, *Coatings* **2022**, *12*, 1115.
- [40] J. Bçcela, M. B. łabowska, J. Detyna, A. Zięty, I. Michalak, *Materials* **2020**, *13*, 3257.
- [41] S. Ouyang, Y. Xie, D. Wang, D. Zhu, X. Xu, T. Tan, H. H. Fong, *J. Nanomater.* **2015**, *2015*, 603148.
- [42] Libretexts, Properties of Gallium Arsenide, accessed: June, **2023**.
- [43] J. Kim, N. Kim, M. Kwon, J. Lee, *ACS Applied Materials Interfaces* **2017**, *9*, 25700.
- [44] J. Kim, G. A. Salvatore, H. Araki, A. M. Chiarelli, Z. Xie, A. Banks, X. Sheng, Y. Liu, J. W. Lee, K.-I. Jang, *Sci. Adv.* **2016**, *2*, e1600418.
- [45] H. Li, Y. Xu, X. Li, Y. Chen, Y. Jiang, C. Zhang, B. Lu, J. Wang, Y. Ma, Y. Chen, *Adv. Healthcare Mater.* **2017**, *6*, 1601013.
- [46] J. Kim, P. Gutruf, A. M. Chiarelli, S. Y. Heo, K. Cho, Z. Xie, A. Banks, S. Han, K. I. Jang, J. W. Lee, *Adv. Funct. Mater.* **2017**, *27*, 1604373.
- [47] H. J. Eun, H. Lee, Y. Shim, G. U. Seo, A. Y. Lee, J. J. Park, J. Heo, S. Park, J. H. Kim, *Isience* **2022**, *25*, 104194.
- [48] T. Yokota, P. Zalar, M. Kaltenbrunner, H. Jinno, N. Matsuhisa, H. Kitanosako, Y. Tachibana, W. Yukita, M. Koizumi, T. Someya, *Sci. Adv.* **2016**, *2*, e1501856.
- [49] G. Simone, D. Tordera, E. Delvitto, B. Peeters, A. J. Van Breemen, S. C. Meskers, R. A. Janssen, G. H. Gelinck, *Adv. Opt. Mater.* **2020**, *8*, 1901989.
- [50] S. Park, K. Fukuda, M. Wang, C. Lee, T. Yokota, H. Jin, H. Jinno, H. Kimura, P. Zalar, N. Matsuhisa, *Adv. Mater.* **2018**, *30*, 1802359.
- [51] Y. Khan, D. Han, A. Pierre, J. Ting, X. Wang, C. M. Lochner, G. Bovo, N. Yaacobi-Gross, C. Newsome, R. Wilson, *Proc. Natl. Acad. Sci. USA* **2018**, *115*, E11015.
- [52] H. Xu, J. Liu, J. Zhang, G. Zhou, N. Luo, N. Zhao, *Adv. Mater.* **2017**, *29*, 1700975.
- [53] T.-H. Kim, C.-S. Lee, S. Kim, J. Hur, S. Lee, K. W. Shin, Y.-Z. Yoon, M. K. Choi, J. Yang, D.-H. Kim, *ACS Nano* **2017**, *11*, 5992.
- [54] E. O. Polat, G. Mercier, I. Nikitskiy, E. Puma, T. Galan, S. Gupta, M. Montagut, J. J. Piqueras, M. Bouwens, T. Durduran, *Sci. Adv.* **2019**, *5*, eaaw7846.
- [55] H. S. Lee, B. Noh, S. U. Kong, Y. H. Hwang, H.-E. Cho, Y. Jeon, K. C. Choi, *npj Flexible Electron.* **2023**, *7*, 15.
- [56] B. H. Kang, K. Park, M. Hamsch, S. Hong, H. T. Kim, D. H. Choi, J. H. Lee, S. Kim, H. J. Kim, *Nano Energy* **2022**, *92*, 106773.
- [57] H. Chen, Y. Xu, J. Zhang, W. Wu, G. Song, *Nanomaterials* **2019**, *9*, 778.
- [58] Toshiba, What is a wide-band-gap semiconductor?, accessed: June, **2023**.
- [59] Ossila, P. T. B. 7., accessed: June, **2023**.
- [60] B. Xie, Z. Chen, L. Ying, F. Huang, Y. Cao, *InfoMat* **2020**, *2*, 57.
- [61] J. Yuan, Y. Zhang, L. Zhou, G. Zhang, H.-L. Yip, T.-K. Lau, X. Lu, C. Zhu, H. Peng, P. A. Johnson, *Joule* **2019**, *3*, 1140.
- [62] E. Von Hauff, V. Dyakonov, J. Parisi, *Sol. Energy Mater. Sol. Cells* **2005**, *87*, 149.
- [63] P. D. Cunningham, L. M. Hayden, *J. Phys. Chem. C* **2008**, *112*, 7928.
- [64] S. Holliday, R. S. Ashraf, A. Wadsworth, D. Baran, S. A. Yousaf, C. B. Nielsen, C.-H. Tan, S. D. Dimitrov, Z. Shang, N. Gasparini, *Nat. Commun.* **2016**, *7*, 11585.
- [65] I. H. Jung, C. T. Hong, U.-H. Lee, Y. H. Kang, K.-S. Jang, S. Y. Cho, *Sci. Rep.* **2017**, *7*, 44704.
- [66] M. Wang, H. Wang, T. Yokoyama, X. Liu, Y. Huang, Y. Zhang, T.-Q. Nguyen, S. Aramaki, G. C. Bazan, *J. Am. Chem. Soc.* **2014**, *136*, 12576.
- [67] J. Yang, S. Peng, Y. Shi, S. Ma, H. Ding, G. Rupprechter, J. Wang, *J. Catal.* **2020**, *389*, 71.
- [68] B. Moosasait, W. I. Maria Siluvairaj, R. Eswaran, *IET Sci. Measure. Technol.* **2021**, *15*, 527.
- [69] S. W. Kim, S. Park, S. Lee, D. Kim, G. Lee, J. Son, K. Cho, *Adv. Funct. Mater.* **2021**, *31*, 2010870.
- [70] J.-H. Lee, S.-J. Park, J.-W. Choi, *Nanomaterials* **2019**, *9*, 297.
- [71] G. Suganya, M. Arivanandhan, G. Kalpana, *Mater. Sci. Semicond. Process.* **2022**, *148*, 106789.
- [72] S. Talam, S. R. Karumuri, N. Gunnam, *Int. Schol. Res. Not.* **2012**, *2012*, 372505.
- [73] Y. Zhang, J. Chen, B.-S. Sun, S. Liu, Z.-J. Wang, S.-H. Liu, Y.-C. Shu, J.-L. He, *J. Central South Univ.* **2022**, *29*, 1062.
- [74] M. Grzybowski, D. T. Gryko, *Adv. Opt. Mater.* **2015**, *3*, 280.
- [75] P. Wang, Z. Lin, X. Su, Z. Tang, *Nano Today* **2017**, *12*, 64.
- [76] I. Miranda, A. Souza, P. Sousa, J. Ribeiro, E. M. Castanheira, R. Lima, G. Minas, *J. Funct. Biomater.* **2021**, *13*, 2.

- [77] P. Segers, E. R. Rietzschel, J. A. Chirinos, *Arterioscler. Thromb. Vasc. Biol.* **2020**, *40*, 1034.
- [78] Y. Maeda, M. Sekine, T. Tamura, *J. Med. Syst.* **2011**, *35*, 829.
- [79] D. Biswas, N. Simões-Capela, C. Van Hoof, N. Van Helleputte, *IEEE Sens. J.* **2019**, *19*, 6560.
- [80] J. Harju, A. Vehkaoja, V. Lindroos, P. Kumpulainen, S. Liuhanen, A. Yli-Hankala, N. Oksala, *J. Clin. Monitor. Comput.* **2017**, *31*, 1019.
- [81] S. Rajala, H. Lindholm, T. Taipalus, *Physiological measurement* **2018**, *39*, 075010.
- [82] T. Ysehak Abay, K. Shafqat, P. A. Kyriacou, *Biosensors* **2019**, *9*, 71.
- [83] B. Vescio, M. Salsone, A. Gambardella, A. Quattrone, *Sensors* **2018**, *18*, 844.
- [84] J. A. Patterson, D. C. McIlwraith, G.-Z. Yang, *Sixth Internat. Workshop on Wearable and Implantable Body Sensor Networks* **2009**, 286.
- [85] M. Anvaripour, M. Khoshnam, C. Menon, M. Saif, *Frontiers in Robotics and AI* **2020**, *7*, 573096.
- [86] C. Sealy, *Nano Today* **2021**, *36*, 101068.
- [87] F. Moggioli, T. Pérez-Fernández, S. Liébana, E. B. Corredor, S. Armijo-Olivo, J. Fernandez-Carnero, R. Raya, P. Conde, O. Rodríguez-López, C. Sánchez, *BMJ Open* **2022**, *12*, e058190.
- [88] A. Pongwisuthiruchte, S. T. Dubas, C. Aumnate, P. Potiyaraj, *Sci. Rep.* **2022**, *12*, 20025.
- [89] J. Li, J. Liu, W. Huo, J. Yu, X. Liu, M. J. Haslinger, M. Muehlberger, P. Kulha, X. Huang, *Materials Today Nano* **2022**, *18*, 100201.
- [90] V. Tewary, Y. Zhang, *Modeling, Characterization, and Production of Nanomaterials: Electronics, Photonics, and Energy Applications*, Woodhead Publishing, xx **2022**.
- [91] A. M. Díez-Pascual, A. Rahdar, *ChemMedChem* **2022**, *17*, 202200142.
- [92] V. Shah, J. Bhaliya, G. M. Patel, K. Deshmukh, *Polym. Adv. Technol.* **2022**, *33*, 3023.
- [93] A. A. Inada, S. Arman, B. Safaei, *J. Energy Storage* **2022**, *55*, 105661.
- [94] S. Li, X. Zhou, Y. Dong, J. Li, *Macromol. Rapid Commun.* **2020**, *41*, 2000444.
- [95] Y. Liu, S. Shang, S. Mo, P. Wang, H. Wang, *Int. J. Prec. Engineer. Manufact.-Green Technol.* **2021**, *8*, 1323.
- [96] S. Z. Homayounfar, T. L. Andrew, *SLAS TECHNOLOGY: Translating Life Sciences Innovation* **2020**, *25*, 9.
- [97] M. Pateraki, K. Fysarakis, V. Sakkalis, G. Spanoudakis, I. Varlamis, M. Maniadakis, M. Lourakis, S. Ioannidis, N. Cummins, B. Schuller, *Wearable Implantable Medical Devices* **2020**, 25.
- [98] D. Verma, K. R. Singh, A. K. Yadav, V. Nayak, J. Singh, P. R. Solanki, R. P. Singh, *Biosen. Bioelectro.: X* **2022**, *11*, 100153.
- [99] J. Zhao, S. Zhang, Y. Sun, N. Zhou, H. Yu, H. Zhang, D. Jia, *ACS Photonics* **2022**, *9*, 2579.
- [100] L. Zhu, J. Zhang, H. Liu, Y. Chu, *Federated Learning and AI for Healthcare 5.0* **2024**, 61.
- [101] S. Liao, H. Liu, W.-H. Lin, D. Zheng, F. Chen, *Front. Physiol.* **2023**, *14*.
- [102] H. Liu, F. Chen, V. Hartmann, S. G. Khalid, S. Hughes, D. Zheng, *Physiol. Meas.* **2020**, *41*, 094001.
- [103] M. Elgendi, R. Fletcher, Y. Liang, N. Howard, N. H. Lovell, D. Abbott, K. Lim, R. Ward, *NPJ Digit. Med.* **2019**, *2*.
- [104] S. Gupta, A. Singh, A. Sharma, R. K. Tripathy, *IEEE Sensors Letters* **2022**, *6*, 1.
- [105] S. G. Khalid, S. M. Ali, H. Liu, A. G. Qurashi, U. Ali, *Med. Biol. Eng. Comput.* **2022**, *60*, 3057.
- [106] N. Baig, *Composites, Part A* **2022**, *165*, 107362.
- [107] A. M. Díez-Pascual, *Materials* **2022**, *15*, 3251.
- [108] B. Peng, F. Zhao, J. Ping, Y. Ying, *Small* **2020**, *16*, 2002681.
- [109] P. Cheng, D. Wang, P. Schaaf, *Adv. Sustainable Syst.* **2022**, *6*, 2200115.
- [110] K. Srivastava, S. Choudhary, A. Sharma, A. Mishra, *Int. Confer. Artif. Intellig. Smart Commun. (AISC)* **2023**, 22.



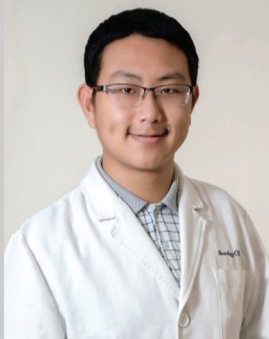
Jinu Mathew is currently doing PhD in developing highly stretchable and conductive next-generation photoplethysmography sensing technology using advanced materials at Coventry University. He received his bachelor's degree in mechanical engineering from VTU, India and master's degree in Nanotechnology from KTU, India. He also holds a MSc degree in Advanced Mechanical Engineering from Coventry University, UK.



Dingchang Zheng received his BS degree in biomedical engineering from Zhejiang University, China, and his PhD degree in medical physics from Newcastle University, UK. He is currently a professor of healthcare technology and a research theme leader with Coventry University. He is the winner of the IPeM Martin Black Annual Prize (2011) and the Institution of Engineering and Technology (IET) JA Lodge Award 2009 for Recognizing and Promoting Outstanding Work in the Field of Research and Development in Medical Engineering



Jianwei Xu is a Principal Scientist at A*STAR's Institute of Materials Research and Engineering (IMRE), and an adjunct Associate Professor at the National University of Singapore (NUS). Xu received his PhD from NUS. At IMRE, he leads a research group that focuses on electrochromic conjugated polymers, thermoelectric materials, polyhedral oligomeric silsesquioxanes (POSS)-based functional hybrid materials and aggregation-induced emission-based materials.



Haipeng Liu received his BS and MS degrees in electrical engineering and biomedical engineering from Zhejiang University, Hangzhou, China in 2012 and 2015, respectively, and his PhD degree in medical sciences from the Chinese University of Hong Kong, in 2018. From 2019 to 2020, he was a research fellow with the Medical Technology and Research Center, Anglia Ruskin University. Since 2020, he has been a research fellow with Coventry University, UK. He is the author of 60 journal articles and seven conference papers. His research interests include biomechanics, physiological measurement, and simulation of cardiovascular diseases.